RSC Advances

PAPER

View Article Online
View Journal | View Issue

Cite this: *RSC Adv.*, 2020, **10**, 38328

Synthesis, study of antileishmanial and antitrypanosomal activity of imidazo pyridine fused triazole analogues†

Adinarayana Nandikolla,[a] Singireddi Srinivasarao,[a] Banoth Karan Kumar,[b] Sankaranarayanan Murugesan,[b] Himanshu Aggarwal,[a] Louise L. Major,[c] Terry K. Smith[c] and Kondapalli Venkata Gowri Chandra Sekhar *[a]

Received 15th September 2020
Accepted 13th October 2020

DOI: 10.1039/d0ra07881f

rsc.li/rsc-advances

Four groups, thirty-five compounds in total, of novel 1,2,3-triazole analogues of imidazo-[1,2-*a*]-pyridine-3-carboxamides were designed and synthesized using substituted pyridine, propargyl bromide, 2-azidoethyl 4-methyl benzenesulfonate and substituted acetylenes. These compounds were characterized using ^{1}H NMR, ^{13}C NMR, LCMS and elemental analyses and a crystal structure was obtained for one of the significantly active compounds, **8f**. All the synthesized and characterized compounds were screened *in vitro* for antileishmanial and antitrypanosomal activity against *Leishmania major* and *Trypanosoma brucei* parasites, respectively. Among the tested analogues, five compounds (**8d**, **8f**, **8j**, **10b** and **10d**) exhibited significant antileishmanial activity while three compounds (**10b**, **11a** and **11b**) showed substantial activity against *T. brucei* parasite. *In silico* ADME prediction studies depicted that the essential compounds obeyed Lipinski's rule of five. The predicted *in silico* toxicity profile suggested that the tested compounds would be non-toxic, which was confirmed experimentally by the lack of cytotoxicity against HeLa cells. Finally, a molecular docking study was also performed, for **10d** the most active antileishmanial compound, to study its putative binding pattern at the active site of the selected leishmanial trypanothione reductase target.

1. Introduction

Leishmaniasis is one of the most neglected tropical diseases as identified by the WHO.[1] Over twenty species of protozoan parasites cause the disease and it is transmitted to its mammalian host *via* the bite of ninety different sandfly species. Mostly leishmaniasis affects the developing countries and underprivileged people across the globe. Leishmaniasis was discovered by William Leishman and Charles Donovan in the year 1900 and was observed in the spleen of the patient.[2] If a person is infected with *Leishmania*, treatment is not easy and if it affects immunocompromised patients co-infected with HIV, then the treatment becomes much harder and risky. *Leishmania* is categorized into four classes: (a) cutaneous leishmaniasis (CL), (b) mucocutaneous leishmaniasis (ML), (c) visercal leishmaniasis (VL) and (d) post-kala-azar dermal leishmaniasis (PKDL).[3] The current drugs used for treating leishmaniasis include sodium stibogluconate, itraconazole, paromomycin, miltefosine, amphotericin B, pentamidine, sitamaquine and rifampicin.[4] Most of these drugs were discovered in the middle of the last century and use of them is constantly leading to problematic resistance in several *Leishmania* species. A recent pilot study conducted in India with thirty-eight patients, proved the efficacy of the miltefosine–paromomycin combination in treating PKDL, whose current treatment is lengthy, costly, time consuming and associated with a variety of side-effects.[5] Human African trypanosomiasis also known as "sleeping sickness" is a vector-borne disease mainly caused by infection with protozoan parasites belonging to the genus *Trypanosoma* either *Trypanosoma brucei gambiense* or *Trypanosoma brucei rhodesiense*. Out of this, *Trypanosoma brucei gambiense* is found in twenty-four countries in west and central Africa. This form, currently accounts for 98% of reported cases of sleeping sickness and causes a chronic infection. A person can be infected for months or even years without major signs or symptoms of the disease. Unlike the above, *Trypanosoma brucei rhodesiense* is found in thirteen countries in eastern and southern Africa. Nowadays, this form represents under 2% of reported cases and causes an acute infection. First signs and symptoms are

[a]*Department of Chemistry, Birla Institute of Technology and Science, Pilani, Hyderabad Campus, Jawahar Nagar, Kapra Mandal, Hyderabad – 500078, Telangana, India. E-mail: kvgc@hyderabad.bits-pilani.ac.in; kvgcs.bits@gmail.com; Tel: +91 40 66303527*

[b]*Medicinal Chemistry Research Laboratory, Department of Pharmacy, Birla Institute of Technology and Science Pilani, Pilani Campus, Pilani-333031, Rajasthan, India*

[c]*Schools of Biology & Chemistry, BSRC, The University, St. Andrews, Fife, Scotland KY16 9ST, UK*

† Electronic supplementary information (ESI) available. CCDC 1991585. For ESI and crystallographic data in CIF or other electronic format see DOI: 10.1039/d0ra07881f

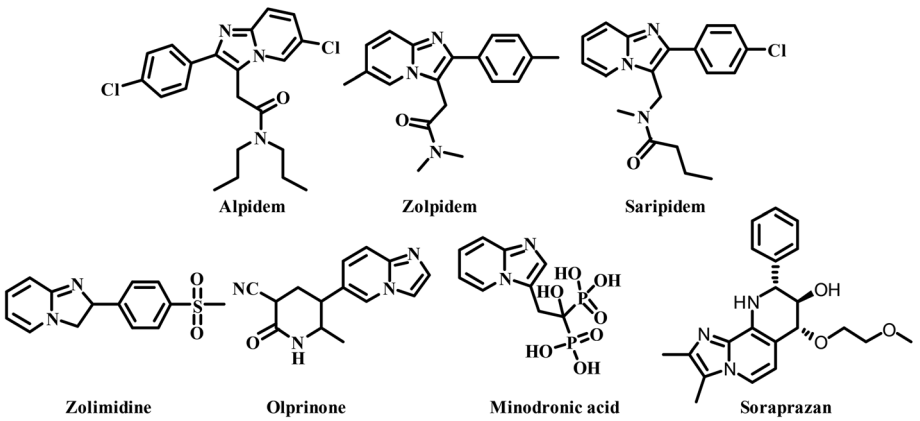

Fig. 1 Imidazo-[1,2-*a*]-pyridine based drugs.

observed within few months or weeks after infection. In general, it involves two stages, in the first stage (also called haemo-lymphatic stage), the trypanosomes multiply in subcutaneous tissues, blood and lymph. This entails bouts of fever, headaches, enlarged lymph nodes, joint pains and itching. In the second stage (known as the neurological or meningo-encephalic stage), the parasites cross the blood–brain barrier to infect the central nervous system. This is where more obvious signs and symptoms of the disease appear: changes of behaviour, confusion, sensory disturbances and poor coordination as well as disturbance of the sleep cycle. They are transmitted to humans by tsetse fly (*Glossina* genus) bites. It is endemic in thirty-seven sub-Saharan African countries where it has threatened millions of people. Without treatment, the disease is considered fatal as tsetse flies transmit the disease. Since the number of new human African trypanosomiasis cases reported between 2000 and 2018 dropped by 95%, the WHO neglected tropical diseases road map targeted its elimination as a public health problem by 2020 and eradication by 2030.[6]

The imidazo-[1,2-*a*]-pyridine moiety already exists in several pharmacologically significant molecules. This core moiety is found in many pharmaceutical compounds that display benzodiazepine receptor agonism, antifungal, antitumor, antiviral, antibacterial, analgesic, and anti-HIV properties.[7–9] The imidazo-[1,2-*a*]-pyridine core is present in some established drugs (Fig. 1), such as alpidem (anxiolytic),[10] zolpidem (hypnotic),[11] saripidem (sedative and anxiolytic),[12] zolimidine (anti-ulcer),[13] olprinone (to treat acute heart failure),[14] minodronic acid (to treat anxiety, heart failure, osteoporosis),[15] and Soraprazan (anti-ulcer).[16] It is also present in some biologically active derivatives such as GSK812397 (CXCR4 antagonist),[17] PI3K-α inhibitors,[18] positive allosteric modulators of mGlu2 receptors,[19] TNF-α inhibitors (Fig. 2).[20]

Castera-Ducrosteam reported imidazo-[1,2-*a*]-pyridine based analogues as antileishmanial agents. From this work, forty-four compounds are tested for *Leishmania donovani* promastigotes. Four selective hit compounds exhibited IC_{50} values 12.6, 18.2, 14.0 μM, and compound **A** (Fig. 3) with an IC_{50} 1.8 μM, was the most active one of the series.[21] Cyril Fersing's team reported twenty-nine compounds with good antileishmanial activity against *L. donovani*, *L. infantum* and *L. major* forms of promastigote and amastigote. Compound **B** (Fig. 3), showed IC_{50} = 1–2.1 μM and has low cytotoxicity against the human HepG2 cell line (CC_{50} > 100 μM). The IC_{50} values of the compound **C** (Fig. 3) were 1.2 and 2.3 μM against *L. donovani* of promastigote and intramacrophase of amastigotes, respectively.[22] John J. Allocco team did the work on whole-cell growth inhibitors of casein kinase 1 (CK 1) of the *L. major* and *T. brucei* parasites. The compounds **D** and **E** (Fig. 3) showed growth inhibition with IC_{50} values of 0.5 and 0.2 μM against *L. major* while *in vitro* CK1 activity with IC_{50} values of 9.0 and 8.0 nM respectively was observed.[23] Marhadour *et al.* reported that the diarylimidazo-[1,2-*a*]-pyridines exhibited low cytotoxicity against the HeLa cells. Compound **F** was the most potent one against the promastigote form of *L. major* with IC_{50} of 4.0 μM (Fig. 3).[24]

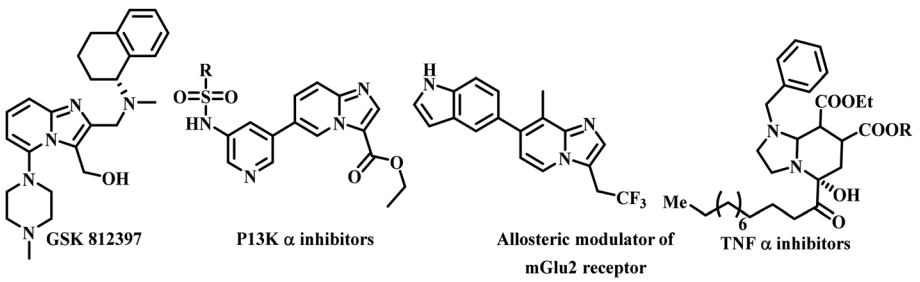

Fig. 2 Biologically active imidazo-[1,2-*a*]-pyridine derivatives.

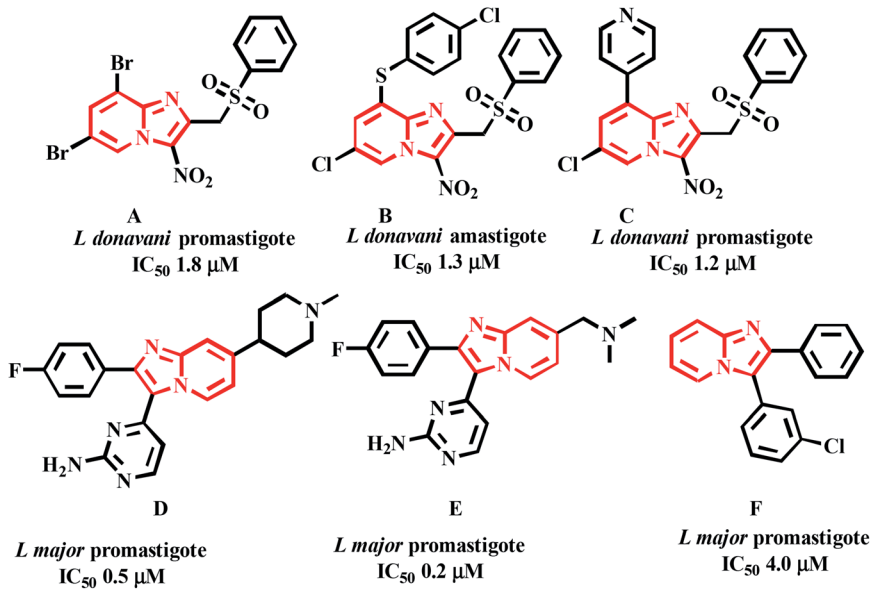

Fig. 3 Imidazo-[1,2-*a*]-pyridine based derivatives as antileishmanial agents.

Several triazole containing drugs are currently available in the market. They exhibit pharmacological activities such as antileishmanial, anticancer, antimalarial, antitubercular, *etc.*[25–28] Mubritinib is used for breast, bladder, kidney, and prostate cancers.[29] The compound carboxyamidotriazole or CAI is an anticancer drug currently in phase III clinical trials.[30,31] *tert*-Butyldimethylsilyl-spiroaminooxathioledioxide (**TSAO**) is used as an anti-HIV reverse transcriptase inhibitor.[32] Cefatrizine and tazobactam are used as antibiotics,[33] while rufinamide is used as an anticonvulsant (Fig. 4).[34]

Casemate *et al.* reported sixteen 1,4-diaryl-1,2,3-triazole analogues. From this work, two compounds showed best *in vitro* activity against *L. amazonensis* promastigotes with IC_{50} values of 1.1 μM and 3.71 μM. Compound **G** (Fig. 5) showed activity against both *L. amazonensis* and *L. infantum* with IC_{50} values of 7.23 μM and 5.2 μM.[35] Dwivedi team reported eighteen triazole based benzylquercetin glycoconjugates that showed activity against the promastigotes and amastigotes of *Leishmania donovani*. In this work, compound **H** (Fig. 5) showed the best activity with IC_{50} values 7.76 μM and 6.08 μM respectively.[36] Tahghighi *et al.* reported fourteen thiadiazol-2-amine containing triazole analogues. From this work, compound **I** (Fig. 5) was the most active one against the promastigotes forms of *L. major* with IC_{50} 12.2 μM.[37] Guimarães team synthesized lapachone based 1,2,3-triazoles and evaluated in different resistant strains of *L. infantum* and *L. amazonensis*. Compound **J** (Fig. 5) showed activity in wild type with $IC_{50} \sim 1.00$ μM and 1.11 μM against *L. infantum* and *L. amazonensis*; in antimony-resistant (2700R) strain IC_{50} of 1.04 μM and 1.03 μM was observed in both *L. infantum* and *L. amazonensis* respectively.[38] Mohammad Masood's team reported eighteen amino acid-triazole derivatives. From this work, compound **K** (Fig. 5) showed moderate activity against the promastigote form of *L. donovani* (Dd8 strain) with IC_{50} 88.33 μM.[39] Chris Marie team synthesized hydroquinone-

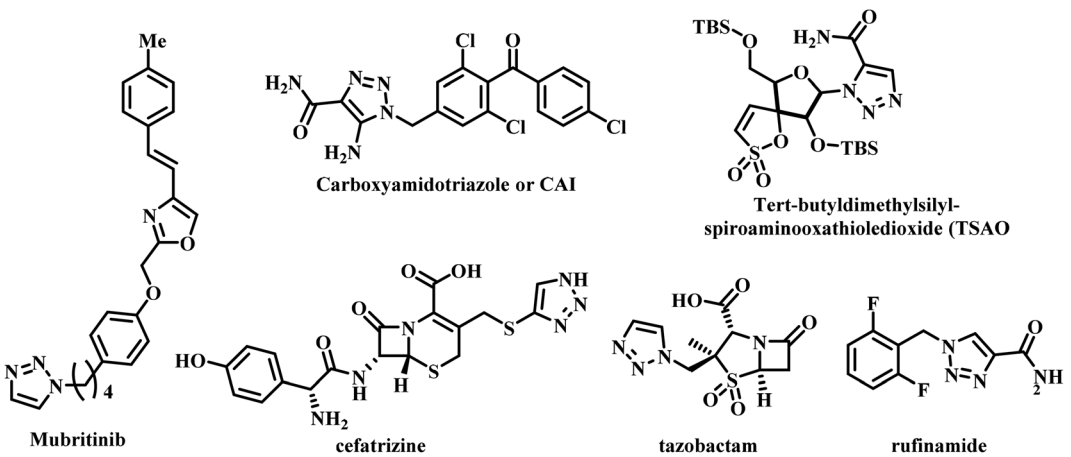

Fig. 4 Triazole containing drugs.

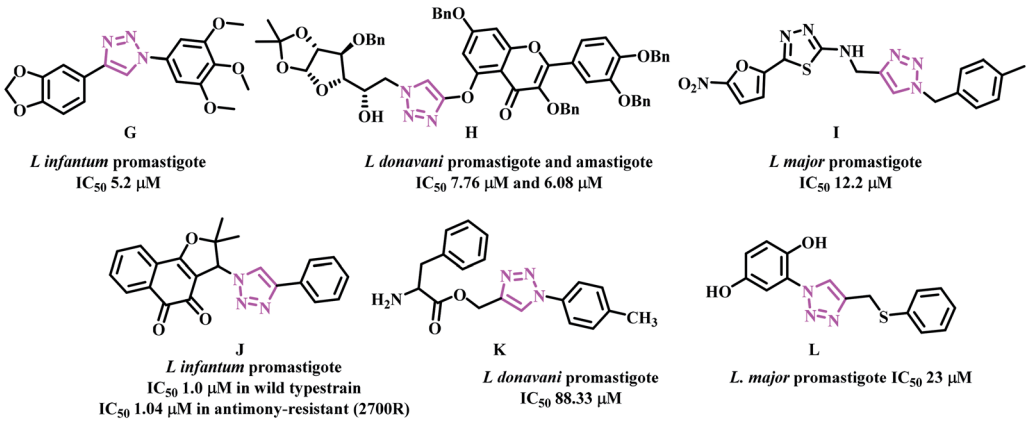

Fig. 5 Triazole based antileishmanial analogues.

triazole based eleven compounds and compound **L** with IC_{50} 23 μM against *L. major* promastigote form was the most active one. Further, these compounds were found to be non-toxic against human embryonic kidney cells (Fig. 5).[40]

Piperazine is another attractive scaffold that has a multitude of pharmacological effects and is also used as a linker in several drug molecules. It is present in numerous marketed drugs such as ranolazine (antianginal), imatinib (anticancer), buspirone (antidepressant), cinnarazine (antihistamine), flupentixol (antipsychotic), sildenafil (erectile dysfunction), to name a few.[41] Literature reports indicate that piperazine is used as a linker in obtaining significantly active antileishmanial compounds. Especially acyl group adjacent to the piperazine N was noticed in several active compounds. Alireza *et al.* synthesized 1-[5-(5-nitrofuran-2-yl)-1,3,4-thiadiazole-2-yl]-4-benzoyl piperazine derivatives. From this work, compounds **M** and **N** (Fig. 6) exhibited good activity with IC_{50} 94 and 77.6 μM values against *L. major*'s promastigote form.[42] Carlos Barea *et al.* synthesized 2-cyano-3-(4-phenylpiperazine-1-carboxamido) quinoxaline 1,4-dioxide derivatives. Compound **O** (Fig. 6) with IC_{50} 5.7 μM against axenic forms of *Leishmania infantum* emerged from this work to be the most active compound.[43] Fardmoghadam *et al.* reported furan and thiophene containing 1,3,4-thiadiazole and arylpiperazine based compounds and monitored anti-leishmanial activity against both promastigote and amastigote forms of *Leishmania major*. In this work, compound **P** (Fig. 6) displayed significant activity against promastigote form of *L. major* with IC_{50} 10.73 μM.[44] Chandar *et al.* synthesized various piperazine linked phenyl derivatives and tested them against promastigote and amastigote forms of *L. infantum*. Compound **Q** with IC_{50} values of 3.61 and 44.14 μM against both the forms was the most active compound (Fig. 6).[45]

In the current work, we focused mainly on our efforts towards a synthetic approach implicating the combination of the pharmacophore units of imidazo[1,2-*a*]pyridine, piperazine and triazole (Fig. 7) into one framework. Both imidazo[1,2-*a*]pyridine and the 1,2,3-triazole moiety were linked together by carbonyl piperazine.

2. Results and discussion

2.1 Synthesis

4-Methyl pyridine-2-amine (**1a**) and 5-chloropyridin-2-amine (**1b**) on treatment with ethyl 2-chloro-3-oxobutanoate in DME under reflux for 24 h yielded ethyl-2,7-dimethylimidazo[1,2-*a*] pyridine-3-carboxylate (**2a**) and ethyl-6-chloro-2-methylimidazo [1,2-*a*]pyridine-3-carboxylate (**2b**) respectively.[46] Further reaction of ethyl ester with LiOH in ethanol and water at 70 °C for 12 h afforded substituted carboxylic acids (**3a–b**).[46] The acids **3a** and **3b** on coupling with 1-Boc-piperazine using EDC·HCl,

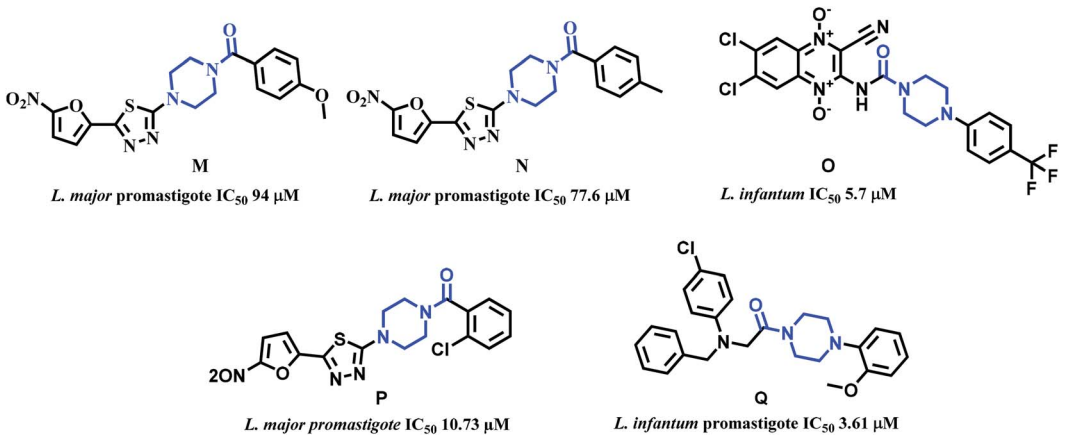

Fig. 6 Piperazine linked antileishmanial derivatives.

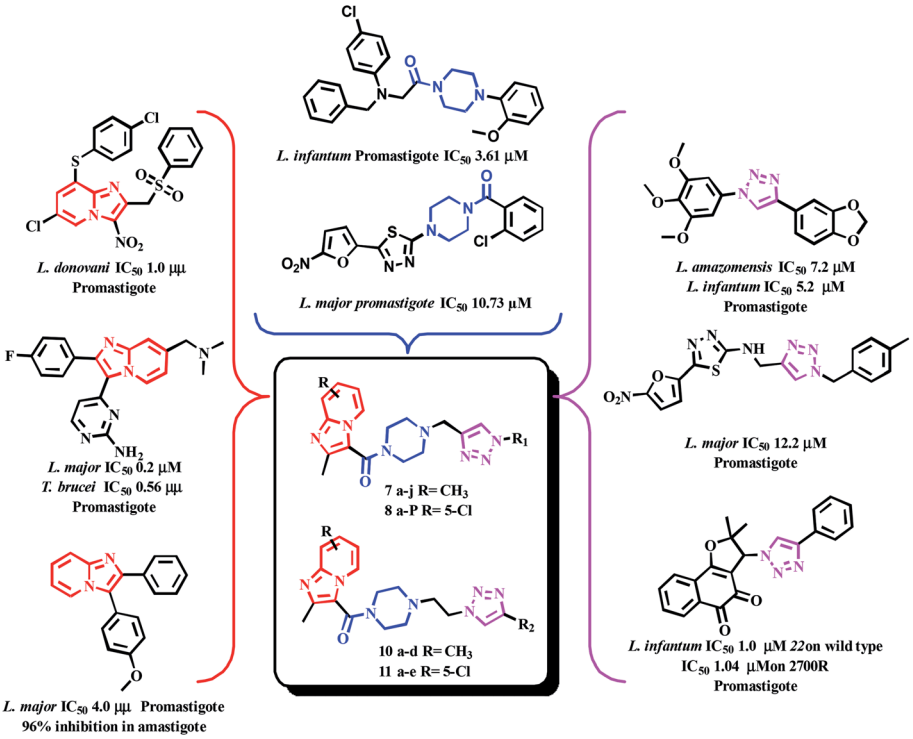

Fig. 7 Design of the titled compounds **7a–j**, **8a–p**, **10a–d**, and **11a–e**.

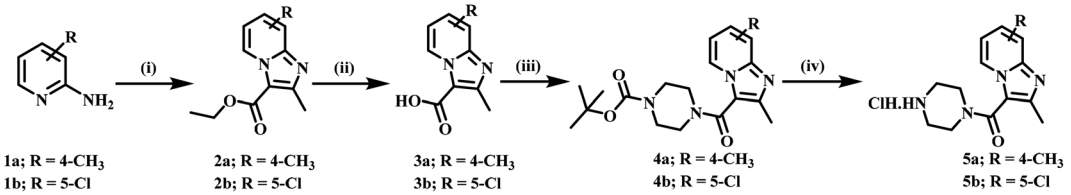

Scheme 1 Preparation of intermediate compounds **5a** and **5b**. Reagents and conditions: (i) **1a**/**1b** (1.0 eq.), ethyl 2-chloro-3-oxobutanoate (1.5 eq.), 1,4-dioxane, reflux, 36 h; (ii) LiOH (2.0 eq.), EtOH, water, 75 °C, 22 h; (iii) 1-Boc-piperazine (1.1 eq.), EDC·HCl (1.5 eq.), hydroxybenzotriazole (1.5 eq.), DIPEA (3 eq.) DMF, rt, 16 h; (iv) 4 M dioxane–HCl (2V) DCM, 0 °C to rt, 4 h.

HOBt, and DIPEA in DMF at rt for 12 h yielded **4a** and **4b**, respectively. The key intermediate **5a** and **5b** were prepared by BOC deprotection of **4a** and **4b** using 4 M dioxane–HCl at 0 °C to rt for 4 h, as shown in Scheme 1. We prepared the title compounds **7a–j** and **8a–p** in two steps, as shown in Scheme 2. First, we performed the S_N2 reaction, involving the reaction of **5a** and **5b** with propargyl bromide, potassium carbonate, and a catalytic amount of potassium iodide in acetone and water at 50 °C for 24 h yielding **6a** and **6b**. Further, **6a** and **6b** on the treatment with various substituted azides using $CuSO_4 \cdot 5H_2O$ and sodium ascorbate in DMF and water at rt to 55 °C for 12 h afforded the title compounds **7a–j** and **8a–p**.

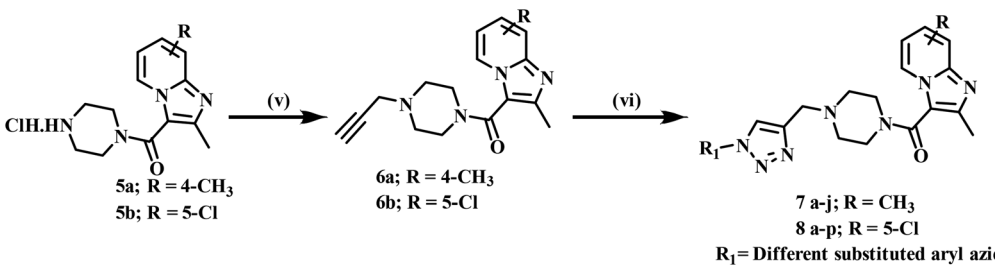

Scheme 2 Preparation of title compounds **7a–j** and **8a–p**. Reagents and conditions: (v) **5a**/**5b** (1.0 eq.), propargyl bromide (80% in toluene) (1.5 eq.), K_2CO_3 (4 eq.), DMF, 100 °C, 12 h; (vi) substituted azides (1.5 eq.), $CuSO_4 \cdot 5H_2O$, (10 mol%), sodium ascorbate (10 mol%), DMF : water (8 : 2), rt, 7–12 h.

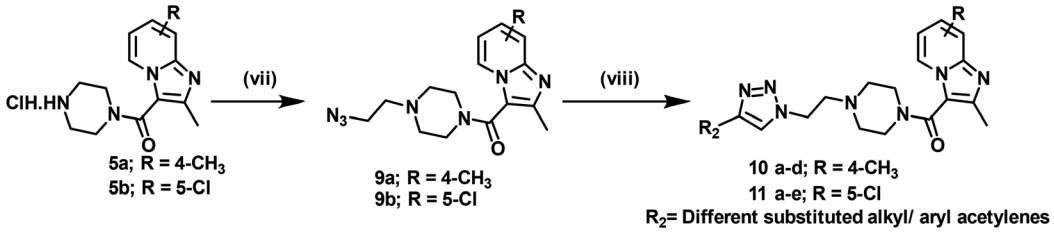

Scheme 3 Preparation of title compounds **10a–d** and **11a–e**. Reagents and conditions: (vii) **5a**/**5b** (1.0 eq.), 2-azidoethyl 4-methylbenzenesulfonate (1.5 eq.), K_2CO_3 (4 eq.), DMF, 100 °C, 12 h; (viii) substituted terminal alkynes (1.5 eq.), $CuSO_4{\cdot}5H_2O$, (10 mol%), sodium ascorbate (10 mol%), DMF : water (8 : 2), rt, 7–12 h.

We prepared the compounds **10a–d** and **11a–e** in two steps, as shown in Scheme 3. Compounds **5a** and **5b** on treatment with 2-azidoethyl 4-methylbenzenesulfonate using K_2CO_3 and a catalytic amount of KI in acetone and water at 50 °C for 24 h yielded **9a** and **9b**. Finally, **9a** and **9b** on treatment with various substituted acetylenes using $CuSO_4 \cdot 5H_2O$ and sodium ascorbate in DMF and water at rt to 55 °C for 12 h afforded the compounds **10a–d** and **11a–e**. All the final compounds were purified by column chromatography using 65–95% ethyl acetate in hexane and 2–6% methanol in CH_2Cl_2 as eluents.

The ^{1}H NMR of final compounds **7a–j**, **8a–p**, **10a–d**, and **11a–e** showed one singlet and one multiplet between δ 3.0–4.00 ppm due to methylene protons between the piperazine-triazole nucleus and piperazine (methylene groups) respectively. Another singlet was observed in the range δ 2.00–2.65 ppm due to methyl protons attached to the imidazole ring. In the aromatic region, one singlet appeared between δ 8.50–9.50 ppm due to the single proton of the triazole nucleus of the compounds **7a–j**, **8a–p**, **10a–d**, and **11a–e** confirming the formation of products. All the synthesized compounds were confirmed by mass spectrometry, ^{1}H and ^{13}C NMR, and elemental analyses.

2.2 Cytotoxicity evaluation

Initially, all the synthesized final compounds were evaluated for cytotoxicity against HeLa cell lines at 100 μM by an Alamar blue assay, which showed most of these compounds were non-toxic to HeLa cells at tested concentration. Compounds that showed cytotoxicity against HeLa cells were further evaluated to determine cytotoxic concentration (CC_{50}) value. Among the tested derivatives, only compounds **8d** and **10b** showed moderate cytotoxicity (CC_{50} 58.09 and 62.67 μM, respectively) against HeLa cells.

2.3 *In vitro* antileishmanial and antitrypanosomal activity of the titled compounds

In the current study, the effect of all synthesized title compounds on promastigotes of *L. major* and trypanocidal properties on bloodstream-form *T. brucei* was evaluated *in vitro* initially as a single point. All compounds with IC_{50} below 75 μM were further tested in replicates of four to obtain a mean and standard deviation. The antileishmanial and antitrypanosomal activities of these novel compounds are shown in Table 1.

Among the tested four series of thirty-five compounds, five compounds (**8d**, **8f**, **8j**, **10b**, and **10d**) showed significant inhibition on the growth of promastigote forms of *L. major* with IC_{50} values in the range of 15 to 47 μM. The most significantly active compound **10d** showed comparable IC_{50} value (15.1 μM) as standard drug miltefosine (12.6 μM). Apart from this, around nine compounds (**7d**, **8c**, **8e**, **8h**, **8k**, **8l**, **8n**, **8o**, and **11b**) exhibited moderate activity against the tested strain of *L. major* with IC_{50} values in the range of 63 to 91 μM. The remaining compounds were found weakly active against the tested forms of the parasite in comparison to the standard drug. Finally, among the four tested series, the majority of **8a–p** and **10a–d** compounds possessed significant activity against the tested strain of promastigote of *L. major* and **7a–j**, **11a–e** series compounds exhibited weak activity against *L. major*. On the other side, among the tested thirty-five compounds, three compounds (**10b**, **11a**, and **11b**) showed significant activity against the *T. brucei* parasite with IC_{50} values of 5.5, 7.4, and 0.7 μM, respectively. The later compound **11b** showed only a ten-fold high IC_{50} value than that of standard drug melarsoprol (0.05 μM). Apart from this, around twelve compounds (**7j**, **8c**, **8d**, **8f**, **8h**, **8i**, **8j**, **8l**, **8n**, **8o**, **8p**, **10a**) exhibited moderate antitrypanosomal activity with IC_{50} values in the range of 23 to 53.9 μM. Around five compounds (**7c**, **7d**, **8e**, **8k**, and **10c**) possessed weak activity with IC_{50} values in the range of 61 to 95.9 μM against the tested *T. brucei* parasite in the *in vitro* assay. The remaining compounds were found largely inactive against the tested forms of the parasite in comparison to the standard drug. In summary, compound **10b** showed significant, and five compounds (**8c**, **8h**, **8l**, **8n**, and **8o**) exhibited moderate activity against both the tested strains of *L. major* and *T. brucei*.

2.4 Structure–activity relationship (SAR) description

Electron withdrawing groups especially at the para position of the phenyl group attached to triazole nucleus (**8d**, **8f**), enhanced the antileishmanial activity. In contrast, a majority of the compounds substituted with electron-withdrawing groups at the *ortho*, *meta*, and *ortho*, *meta* disubstitution (**8h**, **8k**, **8l**, **8n**, **8o**) showed moderate antileishmanial activity against the tested *L. major*. Concerning the antitrypanosomal activity, compounds substituted with bulky group/long chain at the triazole nucleus (**10b** and **11b**) showed significant activity among all the tested series of compounds. Electron-withdrawing groups, especially at the *para* position of the phenyl group attached to the triazole nucleus (**7c**, **7d**, **8e**, **8k**), resulted in a weak antitrypanosomal activity.

2.5 *In silico* prediction of ADME and toxicity parameters

Lipinski's rule of five parameters (mol. weight, donor HB, acceptor HB, and log *P*) of all the titled compounds are satisfied compared

Table 1 Antileishmanial and antitrypanosomal results of the title compounds[a]

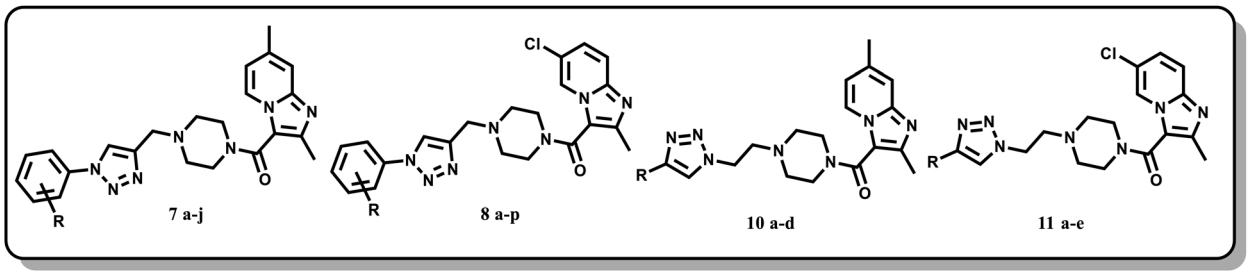

S. no.	Comp. code	R	*L. major* (IC_{50}, μM)	*T. brucei* (IC_{50}, μM)	CC_{50}, μM	SI (*L. major*)	SI (*T. brucei*)
1	**7a**		245.7	131.10	>100	>0.41	>0.76
2	**7b**	4-NO_2	>500	>500	>100	—	—
3	**7c**	4-CF_3	288.3	95.90	>100	>0.35	>1.04
4	**7d**	4-C_2H_5	74.6 ± 1.4	63.2 ± 2.0	>100	>1.49	>1.53
5	**7e**	4-Br	149.2	>500	>100	>0.67	—
6	**7f**	3-NO_2	>250	>500	>100	>0.40	—
7	**7g**	3-OMe	179.8	259.30	>100	>0.56	>0.39
8	**7h**	2-Cl	211.3	>500	>100	>0.47	—
9	**7i**	3-Cl, 4-F	173.8	>500	>100	>0.58	—
10	**7j**	4-OMe, 2-NO_2	114.0	47.7 ± 9.8	>100	>0.88	>2.4
11	**8a**	H	192.4	116.10	>100	>0.52	>0.86
12	**8b**	4-NO_2	>250	>500	>100	>0.40	—
13	**8c**	4-CF_3	62.8 ± 2.4	23.2 ± 1.5	>100	>1.48	>4.3
14	**8d**	4-C_2H_5	**34.5 ± 0.6**	29.1 ± 1.3	58.09	1.57	1.86
15	**8e**	4-F	88.6	94.30	>100	>1.13	>1.06
16	**8f**	4-Br	**33.6 ± 0.6**	28.7 ± 3.1	>100	>2.92	>1.73
17	**8g**	3-NO_2	>250	>500	>100	>0.40	—
18	**8h**	3-CF_3	73.6 ± 2.0	24.2 ± 1.0	>100	>1.43	>2.98
19	**8i**	3-OMe	111.8	50.9 ± 5.7	>100	>0.89	>1.34
20	**8j**	3-Cl	**47.1 ± 0.9**	26.5 ± 1.5	>100	>2.22	>2.36
21	**8k**	2-F	73.1 ± 2.8	61.2 ± 2.5	>100	>1.38	>1.66
22	**8l**	2-Cl	91.48	33.5 ± 2.7	>100	>1.09	>2.03
23	**8m**	3-Cl, 4-F	212.20	>500	>100	>0.47	—
24	**8n**	3,5-CH_3	70.9 ± 2.8	53.90	>100	>1.43	>1.85
25	**8o**	3,4-CH_3	60.9 ± 1.0	40.9 ± 2.0	>100	>1.43	>2.42
26	**8p**	4-OMe, 2-NO_2	100.7	46.3 ± 1.6	>100	>0.99	>2.11
27	**10a**	*n*-Propyl	176.1	40.5 ± 2.7	>100	>0.57	>1.44
28	**10b**	*n*-Nonyl	**38.5 ± 0.9**	**5.5 ± 0.5**	62.67	1.63	6.83
29	**10c**	Cyclopropyl	250.6	71.3	>100	>0.40	>1.40
30	**10d**	4-*t*-Butyl phenyl	**15.1 ± 1.0**	>500	>100	>6.37	—
31	**11a**	*n*-Propyl	475.1	**7.4 ± 0.9**	>100	>0.21	>3.09
32	**11b**	*n*-Nonyl	62.0 ± 2.7	**0.72 ± 0.57**	>100	>1.63	>6.12
33	**11c**	Cyclopropyl	>500	131.9	>100	>0.19	>0.76
34	**11d**	Phenyl	>250	>500	>100	>0.35	—
35	**11e**	4-*t*-Butyl phenyl	171.1	>500	>100	>1.49	>0.76
36	**Miltefosine**		12.6 ± 0.5	—			
37	**Melarsoprol**		—	0.05 ± 0.01			

[a] The values are either a single IC_{50} determination (for compounds with IC_{50} > 75 μM) or mean ± standard deviations ($n = 4$) (for compounds with IC_{50} < 75 μM).

with the marketed approved drugs. The solvent-accessible surface area, aqueous solubility pattern, brain/blood partition coefficient, and the number of rotatable bonds of the titled compounds were found to be in the prescribed range as that of marketed drugs. The Caco-2 permeability of all the compounds except few compounds (**7b**, **7f**, **7j**, **8b**, and **8g**) was found to be moderate when compared to the marketed drugs. Percent of human oral absorption was 100% in the compounds **10b** and **10d**, while in compound **8p**, it is 48%. For the rest of the final compounds, it lies between 84–55% (Table 2).

2.6 *In silico* predicted toxicity profile of the titled compounds

The results of anticipated toxicity studies of the final compounds (**7a–j**, **8a–p**, **10a–d**, and **11a–e**) revealed that the tested compounds are non-toxic. Cancer-causing properties like mutagenicity and tumorigenicity of these agents were found to

Table 2 Results of *in silico* predicted ADME parameters of the titled analogues[a]

S. no.	Comp. code	Mol. wt.	SASA	Donor HB	Acceptor HB	log $P_{o/w}$	log S	P_{Caco}	log BB	Rotor	% Human oral absorption
1	**7a**	415.50	757.26	0.00	8.50	3.07	−4.41	245.81	−0.38	3.00	87.72
2	**7b**	460.49	797.80	0.00	9.50	2.39	−4.49	**34.87**	−1.49	4.00	55.57
3	**7c**	483.50	812.89	0.00	8.50	4.12	−5.98	256.96	−0.12	3.00	94.18
4	**7d**	443.55	821.72	0.00	8.50	3.79	−5.47	256.76	−0.48	4.00	92.25
5	**7e**	494.39	786.30	0.00	8.50	3.66	−5.30	245.73	−0.22	3.00	91.14
6	**7f**	460.49	797.65	0.00	9.50	2.38	−4.49	**33.53**	−1.52	4.00	55.23
7	**7g**	445.52	795.51	0.00	9.25	3.20	−4.58	282.14	−0.40	4.00	89.53
8	**7h**	449.94	778.99	0.00	8.50	3.57	−5.07	274.69	−0.20	3.00	91.50
9	**7i**	467.93	789.71	0.00	8.50	3.84	−5.50	283.04	−0.07	3.00	93.32
10	**7j**	490.52	823.13	0.00	10.25	2.59	−4.42	**56.64**	−1.30	5.00	60.54
11	**8a**	435.92	748.21	0.00	8.50	3.25	−4.54	256.45	−0.18	3.00	89.11
12	**8b**	480.91	789.14	0.00	9.50	2.56	−4.63	**34.89**	−1.31	4.00	56.61
13	**8c**	503.91	802.61	0.00	8.50	4.28	−6.09	256.02	0.06	3.00	82.16
14	**8d**	463.97	812.97	0.00	8.50	4.01	−5.61	291.36	−0.23	4.00	94.52
15	**8e**	453.91	757.74	0.00	8.50	3.50	−4.93	256.01	−0.08	3.00	90.53
16	**8f**	514.81	777.17	0.00	8.50	3.84	−5.43	257.36	−0.02	3.00	79.61
17	**8g**	480.91	788.44	0.00	9.50	2.56	−4.63	**33.38**	−1.32	4.00	56.24
18	**8h**	503.91	800.22	0.00	8.50	4.26	−6.05	243.67	0.04	3.00	81.63
19	**8i**	465.94	787.38	0.00	9.25	3.38	−4.74	281.53	−0.22	4.00	90.56
20	**8j**	470.36	774.46	0.00	8.50	3.82	−5.36	282.23	0.02	3.00	93.17
21	**8k**	453.91	757.34	0.00	8.50	3.54	−4.88	304.91	−0.01	3.00	92.11
22	**8l**	470.36	770.05	0.00	8.50	3.79	−5.21	307.83	0.04	3.00	93.66
23	**8m**	488.35	782.52	0.00	8.50	4.03	−5.68	281.51	0.11	3.00	94.37
24	**8n**	463.97	813.29	0.00	8.50	3.90	−5.78	242.65	−0.26	3.00	92.49
25	**8o**	463.97	805.29	0.00	8.50	3.87	−5.63	243.04	−0.25	3.00	92.29
26	**8p**	510.94	814.65	0.00	10.25	2.77	−4.57	56.18	−1.12	5.00	**48.54**
27	**10a**	395.51	770.01	0.00	9.00	2.69	−3.90	263.71	−0.55	6.00	86.02
28	**10b**	479.67	957.13	0.00	9.00	4.96	−6.47	245.83	−1.11	12.00	100.00
29	**10c**	393.49	697.95	0.00	9.00	2.23	−2.86	257.06	−0.31	4.00	83.11
30	**10d**	485.63	866.91	0.00	9.00	4.46	−5.90	302.69	−0.44	5.00	100.00
31	**11a**	415.93	734.35	0.00	9.00	2.78	−3.53	326.11	−0.21	6.00	88.23
32	**11b**	500.09	947.49	0.00	9.00	5.13	−6.59	246.81	−0.93	12.00	73.90
33	**11c**	413.91	689.03	0.00	9.00	2.40	−3.00	256.07	−0.12	4.00	84.08
34	**11d**	449.94	764.40	0.00	9.00	3.41	−4.43	329.49	−0.11	4.00	91.95
35	**11e**	506.05	882.00	0.00	9.00	4.73	−6.49	270.88	−0.36	5.00	85.20

[a] Comp. code – compound code; mol. wt. – molecular weight (130–725); SASA – solvent accessible surface area (300–1000); donor HB – hydrogen bond donor (0–6); acceptor HB – hydrogen bond acceptor (0–20); log $P_{o/w}$ – partition co-efficient (octanol/water) (−2.0 to 6.50); log S – solubility compound (−6.5 to 0.5 mol dm^{-3}); P_{Caco} – Caco-2 cell permeability in nm s^{-1} (<25 poor, >500 good); log BB – brain/blood partition coefficient (−3.0 to 1.2); rotor – number of rotatable bonds (0 to 15); % human oral absorption – percentage human oral intestional absorption (up to 100).

be nil. The rest of the features like reproductive effect and irritant effects were also found to be none. With these satisfactory results, we conclude that all the predicted ADME and toxicity parameters of the designed compounds displayed productive results. The results disclosed that these compounds might not face any problems during clinical trials.

Table 3 In-depth analysis of the significantly active compound **10d** and co-crystal ligand of PDB-2JK6

Comp. code	Hydrogen bond with distances (Å)	Π–Π interactions with distances (Å)	Gide score (kcal mol^{-1})
10d	SER-14 (2.26) LYS-60 (2.24)	ASP-327 (2.78)	−6.74
Co-crystal ligand (FAD)	SER-14 (2.26) GLY-15 (2.14) ASP-35 (1.86, 2.04) THR-51 (1.82) LYS-60 (2.11) GLY-127 (2.09, 2.13) ASP-327 (1.85, 2.36) THR-335 (2.26)	TYR-198 (5.45)	−16.24

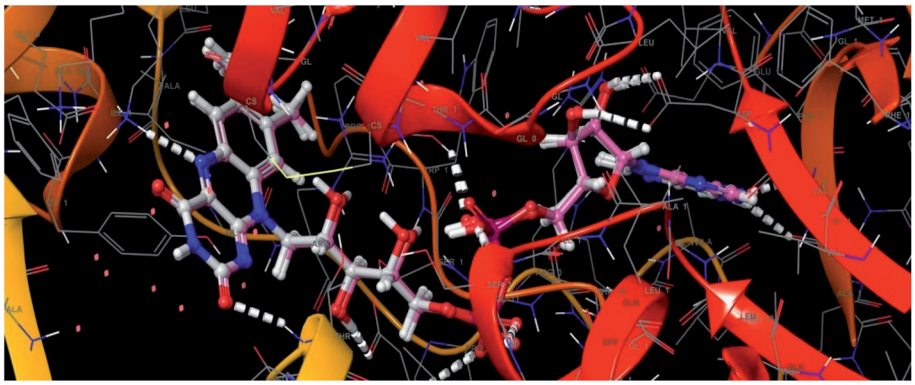

Fig. 8 Superimposed view of the FAD molecule in the active site of the target PDB-2JK6, and its redocked pose in the same target (RMSD – 0.20 Å).

2.7 *In silico* molecular docking studies

To find the putative binding mode of the titled compounds, a docking study was performed, and the results were analyzed (Table 3). The validation of the docking protocol was done by checking the root mean square deviation of the X-ray native pose of the ligand with its docked pose of ligand (Fig. 8) and found to be 0.20 Å. This RMSD could be reliable to proceed for the docking study of the designed scaffolds.

From the docked pose view of extracted co-crystal ligand (Fig. 9), eight hydrogen bond interactions with the amino acid residues SER14, GLY15, ASP35, THR51, LYS60, GLY127, ASP327 and THR335 of the active site of the target protein and one Π–Π interaction with the amino acid residue TYR198 with a docking score value of -16.24 kcal mol^{-1} was observed. The docking score exhibited by the significantly active compound **10d** is -6.74 kcal mol^{-1}. Like co-crystal ligand, compound **10d** also made two hydrogen bond interactions with the amino acid residues SER14, LYS60 and one Π–Π interaction with the amino acid residue ASP327 of the active site of the target protein (Fig. 10). Upon critical examination of the interactions formed by the co-crystal ligand to the target protein and the compound **10d** to the active site amino acid residues of the target protein, it was found that the same amino acid residues (SER14, LYS60) are involved in the similar kind of hydrogen bond interactions with both co-crystal ligand and compound **10d**.

2.8 Single crystal X-ray crystallographic structure of compound 8f

The suitable crystals of compound **8f** for single-crystal X-ray diffraction (SCXRD) study were grown from the mixture of methanol and dichloromethane (1 : 3). The SCXRD measurements were performed on the Rigaku XtaLAB P200 diffractometer using graphite monochromated Mo-Kα radiation (λ = 0.71073 Å). The data was collected and reduced using CrysAlisPro (Rigaku Oxford Diffraction) software. The data collection was carried out at 100 K, and the structures were solved using Olex2 with the ShelX structure solution program using Direct Methods and refined with the ShelXL refinement package using Least Squares minimization. The basic crystallographic data is given in a table in ESI.†

The compound **8f** crystallizes in *Pbca* space group with one linker per asymmetric unit and one molecule of DCM which is disordered over two positions (Fig. 11). The ORTEP diagram of the structure shows that the ellipsoids of all the atoms are well behaved. Crystallographic Data Center and corresponding deposition number is CCDC 1991585.†

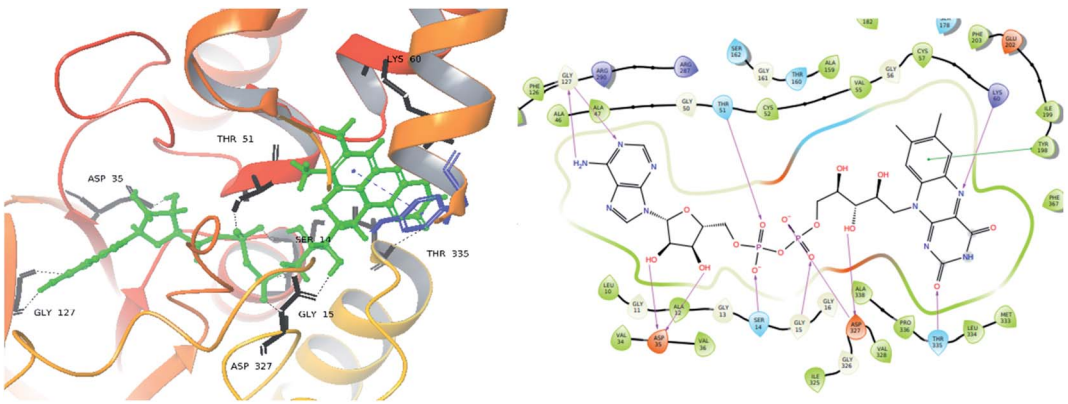

Fig. 9 Exposed amino-acid residue interactions of the FAD molecule in the actives site of the target PDB-2JK6 (black lines – hydrogen bonds, blue – pi interaction in 3D, magenta – hydrogen bond, green – pi interaction in 2D).

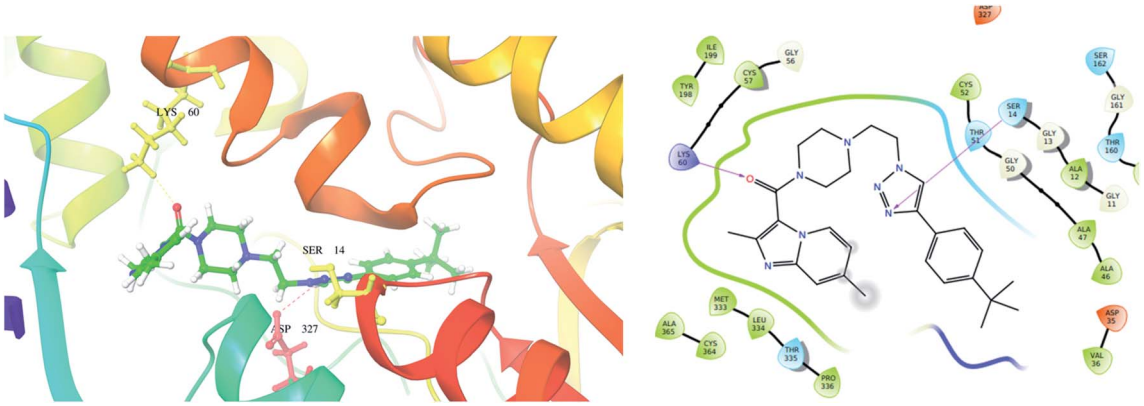

Fig. 10 Exposed amino-acid residue interactions of the significantly active compound **10d** in the actives site of the target PDB-2JK6 (yellow lines – hydrogen bonds, blue – pi interaction in 3D, magenta – hydrogen bond in 2D).

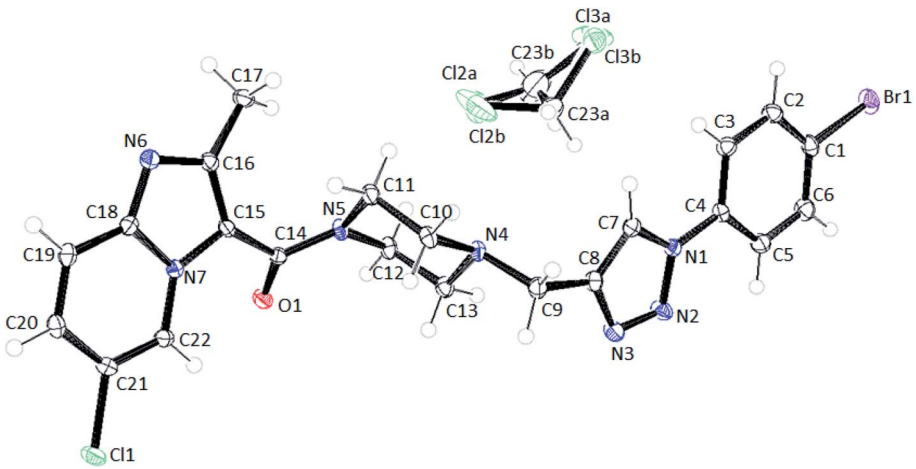

Fig. 11 ORTEP diagram of compound **8f**.

Upon closer look at the structure, it was found that the ligand packs in an interesting manner where the individual units stack antiparallel to each other to minimize the electronic repulsions. The structure show pi–pi stacking between the benzene units of one ligand and the imidazole pyridine units of the other ligand (Fig. 12). The pi–pi stacking distance is in the range of 3.6–3.9 Å.

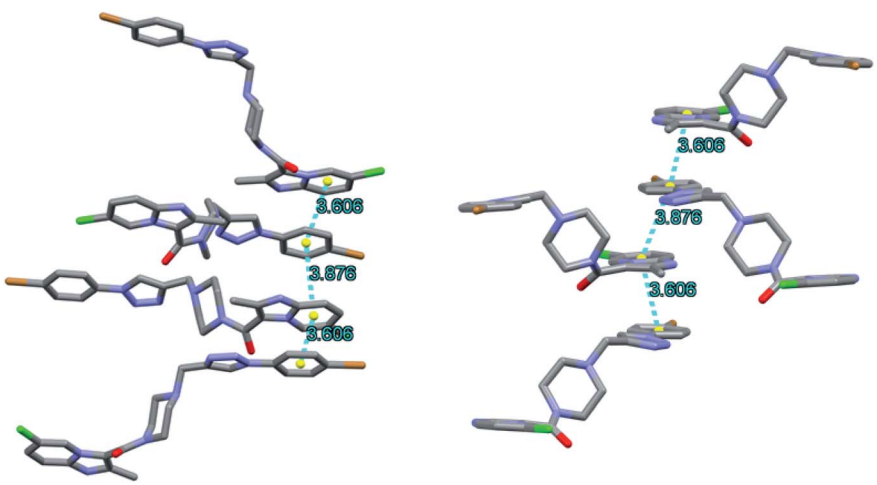

Fig. 12 Packing diagram of **8f** showing pi–pi stacking arrangement as observed along a (left) and c (right) axis.

3. Conclusion

In conclusion, we have designed and synthesized thirty-five novel 1,2,3-triazole analogues of imidazo-[1,2-*a*]-pyridine-3-carboxamides using substituted pyridine, propargyl bromide, 2-azidoethyl-4-methyl benzenesulfonate and substituted acetylenes. The synthesized compounds were well characterized using ^{1}H NMR, ^{13}C NMR, LCMS and elemental analyses. These compounds were further screened *in vitro* for antileishmanial and antitrypanosomal activity against *L. major* and *T. brucei* parasites, respectively. Few compounds exhibited significant to moderate antileishmanial and antitrypanosomal activity in the tested assay system. Five compounds exhibited significant antileishmanial activity (**8d**, **8f**, **8j**, **10b** and **10d**), while three compounds (**10b**, **11a** and **11b**) showed significant activity against the *T. brucei* parasite. *In silico* ADME prediction studies also depicted that the titled compounds do not violate Lipinski's rule of five parameters in comparison with the marketed approved drugs. The predicted toxicity profile also confirmed that the compounds are non-toxic. Finally, molecular docking studies was also performed for significantly active compound (**10d**) in order to study its putative binding pattern at the active site of the selected leishmanial trypanothione reducatse target. The crystal structure developed for one of the significantly active antileishmanial compound **8f** was found to occupy *Pbca* space group. Further, the crystal structure revealed pi–pi stacking between the benzene units of one ligand and the imidazole pyridine units of the other. We also observed that all the final synthesized compounds were non-toxic to HeLa cell line at 100 μM.

4. Experimental section

4.1 Chemistry

The intermediates **2a**, **2b**, **3a**, and **3b** were prepared as per the earlier reported literature protocol.[46] The procedures and the analytical data of the remaining intermediates and final compounds (**7a–j**, **8a–p**, **10a–d**, and **11a–e**) are given in ESI.† The detailed procedures used for cytotoxicity, *in vitro* activity studies, *in silico* toxicity parameters, molecular docking studies, ligand and protein preparation methods, receptor grid generation, docking validation, and docking analysis are also given in ESI.†

4.2 Analytical data of final compounds (7a–j, 8a–p, 10a–d, and 11a–e)

(2,7-Dimethylimidazo-[1,2-*a*]-pyridin-3-yl)(4-((1-phenyl-1*H*-1,2,3-triazol-4-yl)-methyl)-piperazin-1-yl)-methanone (7a). Sticky liquid; (75%); mp 238–240 °C; ^{1}H NMR (400 MHz, DMSO-*d*6) δ 8.74 (s, 1H), 8.35 (d, J = 5.6 Hz, 1H), 7.96–7.87 (m, 2H), 7.60 (dd, J = 10.7, 5.0 Hz, 2H), 7.48 (t, J = 7.4 Hz, 1H), 7.34 (s, 1H), 6.82 (d, J = 7.1 Hz, 1H), 3.73 (s, 2H), 3.56 (s, 4H), 2.53 (d, J = 6.3 Hz, 4H), 2.36 (s, 6H). ^{13}C NMR (101 MHz, DMSO) δ 162.19, 156.46, 144.67, 137.43, 137.15, 130.33, 129.01, 126.49, 122.65, 120.40, 115.27, 115.01, 55.35, 52.89, 45.04, 29.45, 20.83. ESI-MS: (m/z) calcd for $C_{23}H_{25}N_7O$: 415.21, found 416.26 (M + H)$^+$; anal. calcd for $C_{23}H_{25}N_7O$: (%) C, 66.49; H, 6.06; N, 23.60; O, 3.85. Found: C, 66.45; H, 6.10; N, 23.56; O, 3.81.

(2,7-Dimethylimidazo-[1,2-*a*]-pyridin-3-yl)(4-((1-(4-nitrophenyl)-1*H*-1,2,3-triazol-4-yl)-methyl)-piperazin-1-yl)-methanone (7b). Pale yellow solid; (68%); mp 236–238 °C; ^{1}H NMR (400 MHz, DMSO-*d*6) δ 8.96 (s, 1H), 8.45 (d, J = 8.8 Hz, 2H), 8.40 (s, 1H), 8.24 (d, J = 8.8 Hz, 2H), 7.37 (s, 1H), 6.82 (d, J = 6.8 Hz, 1H), 3.74 (s, 2H), 3.56 (s, 4H), 2.61 (d, 4H), 2.35 (s, 6H). ^{13}C NMR (101 MHz, DMSO-*d*6) δ 161.59, 158.42, 151.16, 147.06, 145.51, 141.40, 137.28, 126.78, 126.02, 123.11, 120.92, 115.48, 112.96, 52.91, 52.61, 44.88, 21.25, 15.50. ESI-MS: (m/z) calcd for $C_{23}H_{24}N_8O_3$: 460.49, found 461.00 (M + H)$^+$; anal. calcd for $C_{23}H_{24}N_8O_3$: (%) C, 59.99; H, 5.25; N, 24.33; O, 10.42. Found: C, 59.98; H, 5.65; N, 29.61; O, 5.57.

(2,7-Dimethylimidazo-[1,2-*a*]-pyridin-3-yl)(4-((1-(4-(trifluoro methyl)-phenyl)-1*H*-1,2,3-triazol-4-yl)-methyl)-piperazin-1-yl)-methanone (7c). Pale yellow solid; (71%); mp 200–202 °C; ^{1}H NMR (400 MHz, DMSO-*d*6) δ 8.94 (s, 1H), 8.78 (s, 1H), 8.29 (m, 2H), 7.86 (m, 2H), 7.59 (m, 1H), 6.83 (s, 1H), 3.77 (s, 2H), 3.51 (m, 4H), 2.61 (m, 4H), 2.35 (s, 6H). ^{13}C NMR (101 MHz, DMSO-*d*6) δ 161.46, 159.01, 151.43, 148.18, 146.55, 141.43, 137.64, 126.97, 125.73, 126.07, 122.23, 120.66, 115.93, 113.13, 52.95, 52.63, 44.76, 21.33, 15.41. ESI-MS: (m/z) calcd for $C_{24}H_{24}F_3N_7O$: 483.20, found 484.14 (M + H)$^+$; anal. calcd for $C_{24}H_{24}F_3N_7O$: (%) C, 59.62; H, 5.00; F, 11.79; N, 20.28; O, 3.31. Found: C, 59.65; H, 5.03; F, 11.86; N, 20.25; O, 3.26.

(2,7-Dimethylimidazo-[1,2-*a*]-pyridin-3-yl)(4-((1-(4-ethyl-phenyl)-1*H*-1,2,3-triazol-4-yl)-methyl)-piperazin-1-yl)-methanone (7d). Sticky liquid; (74%); ^{1}H NMR (400 MHz, DMSO-*d*6) δ 8.73 (s, 1H), 8.41 (s, 1H), 7.81 (d, 2H), 7.43 (d, 2H), 6.88 (d, 1H), 3.91 (s, 2H), 3.61 (s, 4H), 2.69 (m, 6H), 2.37 (s, 6H), 1.22 (t, 3H). ^{13}C NMR (101 MHz, DMSO-*d*6) δ 161.82, 144.64, 137.01, 135.43, 130.22, 124.95, 122.43, 122.83, 120.37, 115.91, 52.63, 50.3, 45.06, 27.86, 21.21, 15.47, 14.80. ESI-MS: (m/z) calcd for $C_{25}H_{29}N_7O$: 443.24, found 444.00 (M + H)$^+$; anal. calcd for $C_{25}H_{29}N_7O$: (%) C, 67.70; H, 6.59; N, 22.11; O, 3.61. Found: C, 67.74; H, 6.62; N, 22.07; O, 3.64.

(4-((1-(4-Bromophenyl)-1*H*-1,2,3-triazol-4-yl)-methyl)-piperazin-1-yl)(2,7-dimethylimidazo-[1,2-*a*]-pyridin-3-yl)-methanone (7e). Brown solid; (66%); mp 100–102 °C; ^{1}H NMR (400 MHz, DMSO-*d*6) δ 8.77 (s, 1H), 8.34 (d, 1H), 7.90 (d, 2H), 7.80 (d, 2H), 7.34 (s, 1H), 6.82 (d, 1H), 3.71 (s, 2H), 3.55 (m, 4H), 2.52 (m, 4H), 2.36 (s, 3H), 2.34 (s, 3H). ^{13}C NMR (101 MHz, DMSO-*d*6) δ 162.17, 145.09, 137.43, 136.35, 133.21, 126.65, 122.65, 122.33, 121.72, 115.01, 52.79, 52.63–51.9, 45.06, 21.20, 15.59. ESI-MS: (m/z) calcd for $C_{23}H_{24}BrN_7O$: 493.12, found 494.06 (M + H)$^+$; anal. calcd for $C_{23}H_{24}BrN_7O$: (%) C, 55.88; H, 4.89; Br, 16.16; N, 19.83; O, 3.24. Found: C, 55.85; H, 4.83; Br, 16.19; N, 19.80; O, 3.20.

(2,7-Dimethylimidazo-[1,2-*a*]-pyridin-3-yl)(4-((1-(3-nitrophenyl)-1*H*-1,2,3-triazol-4-yl)-methyl)-piperazin-1-yl)-methanone (7f). Yellow solid; (73%); mp 218–220 °C; ^{1}H NMR (400 MHz, DMSO-*d*6) δ 8.75 (s, 1H), 8.30 (d, 1H), 7.85 (d, 1H), 7.75 (dd, 1H), 7.65 (s, 1H), 7.50 (d, 1H), 7.30 (s, 1H), 6.79 (d, 1H), 3.69 (s, 2H), 3.53 (m, 4H), 2.50 (m, 4H), 2.30 (s, 3H), 2.26 (s, 3H). ^{13}C NMR (101 MHz, DMSO-*d*6) δ 161.61, 157.91, 151.47, 147.28, 145.51, 141.44, 137.84, 126.98, 125.91, 123.10, 120.94, 115.461, 112.34, 110.28, 109.47, 52.92, 52.60, 44.76, 21.24, 15.48. ESI-MS: (m/z) calcd for $C_{23}H_{24}N_8O_3$: 460.20, found 461.24 (M + H)$^+$; anal. calcd for $C_{23}H_{24}N_8O_3$: (%) C,

59.99; H, 5.25; N, 24.33; O, 10.42. Found: C, 60.04; H, 5.21; N, 24.27; O, 10.46.

(2,7-Dimethylimidazo-[1,2-*a*]-pyridin-3-yl)(4-((1-(3-methoxyphenyl)-1*H*-1,2,3-triazol-4-yl)-methyl)-piperazin-1-yl)-methanone (7g). Brown solid; (67%); mp 95–97 °C; ^{1}H NMR (400 MHz, DMSO) δ 8.81 (s, 1H), 8.39 (s, 1H), 7.49 (m, 4H), 7.05 (d, 1H), 6.88 (d, 1H), 3.86 (m, 6H), 3.62 (s, 4H), 2.74 (s, 3H), 2.38 (s, 6H). ^{13}C NMR (101 MHz, DMSO-*d*6) δ 162.93, 161.79, 145.12, 137.64, 136.35, 127.22, 126.61, 126.64, 125.14, 124.32, 122.15, 122.32, 121.77, 115.11, 110.17, 57.63, 52.79, 52.14, 45.06, 21.20, 15.59. ESI-MS: (*m*/*z*) calcd for $C_{24}H_{27}N_7O_2$: 445.22, found 446.16 $(M + H)^+$; anal. calcd for $C_{24}H_{27}N_7O_2$: (%) C, 64.70; H, 6.11; N, 22.01; O, 7.18. Found: C, 64.76; H, 6.05; N, 22.09; O, 7.13.

(4-((1-(2-Chlorophenyl)-1*H*-1,2,3-triazol-4-yl)-methyl)-piperazin-1-yl)(2,7-dimethylimidazo-[1,2-*a*]-pyridin-3-yl)-methanone (7h). Off-white solid; (61%); mp 104–105 °C; ^{1}H NMR (400 MHz, DMSO-*d*6) δ 8.60 (d, 1H), 8.44 (d, 1H), 7.79 (dd, 1H), 7.73–7.59 (m, 4H), 7.44 (d, 1H), 6.96 (d, 1H), 4.14 (s, 2H), 3.65 (m, 4H), 2.89 (m, 4H), 2.41 (s, 6H). ^{13}C NMR (101 MHz, DMSO) δ 161.46, 143.07, 142.32, 140.65, 139.53, 134.82, 132.25, 131.04, 128.97, 128.82, 127.89, 126.89, 126.07, 116.46, 114.13, 52.07, 51.43, 43.83, 21.28, 14.65. ESI-MS: (*m*/*z*) calcd for $C_{23}H_{24}ClN_7O$: 449.17, found 450.10 $(M + H)^+$; anal. calcd for $C_{23}H_{24}ClN_7O$: (%) C, 61.40; H, 5.38; Cl, 7.88; N, 21.79; O, 3.56. Found: C, 61.40; H, 5.42; Cl, 7.92; N, 21.74; O, 3.60.

(4-((1-(3-Chloro-4-fluorophenyl)-1*H*-1,2,3-triazol-4-yl)-methyl)-piperazin-1-yl)(2,7-dimethylimidazo-[1,2-*a*]-pyridin-3-yl)-methanone (7i). Off-white solid; (83%); mp 128–131 °C; ^{1}H NMR (400 MHz, DMSO-*d*6) δ 8.78 (s, 1H), 8.34 (d, 1H), 8.23 (dd, 1H), 7.98 (m, 1H), 7.67 (t, 1H), 7.33 (s, 1H), 6.82 (m, 1H), 3.71 (s, 2H), 3.56 (m, 4H), 2.52 (m, 4H), 2.36 (s, 3H), 2.34 (s, 3H). ^{13}C NMR (101 MHz, DMSO-*d*6) δ 162.05, 158.50, 155.99, 145.03, 137.31, 134.17, 126.44, 122.98, 122.66, 122.34, 121.21, 121.13, 118.69, 118.46, 115.45, 114.98, 52.91, 52.71, 45.10, 21.18, 15.48. ESI-MS: (*m*/*z*) calcd for $C_{23}H_{23}ClFN_7O$: 467.16, found 468.10 $(M + H)^+$; anal. calcd for $C_{23}H_{23}ClFN_7O$: (%) C, 59.04; H, 4.95; Cl, 7.58; F, 4.06; N, 20.95; O, 3.42. Found: C, 59.08; H, 4.90; Cl, 7.62; F, 4.09; N, 20.91; O, 3.47.

(2,7-Dimethylimidazo-[1,2-*a*]-pyridin-3-yl)(4-((1-(4-methoxy-2-nitrophenyl)-1*H*-1,2,3-triazol-4-yl)-methyl)-piperazin-1-yl)-methanone (7j). Pale yellow solid; (69%); mp 98–100 °C; ^{1}H NMR (400 MHz, DMSO-*d*6) δ 8.55 (s, 1H), 8.42 (s, 1H), 7.78 (dd, 2H), 7.50 (dd, 2H), 6.88 (d, 1H), 3.95 (s, 2H), 3.61 (m, 4H), 2.66 (t, 4H), 2.44–2.31 (m, 6H). ^{13}C NMR (101 MHz, DMSO-*d*6) δ 165.24, 160.74, 146.50, 145.52, 138.21, 129.42, 128.06, 126.81, 126.74, 122.52, 119.94, 115.90, 114.81, 111.05, 106.71, 99.39, 57.09, 56.08, 52.41, 44.67, 21.24, 15.29. ESI-MS: (*m*/*z*) calcd for $C_{24}H_{26}N_8O_4$: 490.21, found 491.17 $(M + H)^+$; anal. calcd for $C_{24}H_{26}N_8O_4$: (%) C, 58.77; H, 5.34; N, 22.84; O, 13.05. Found: C, 58.72; H, 5.31; N, 22.80; O, 13.08.

(6-Chloro-2-methylimidazo-[1,2-*a*]-pyridin-3-yl)(4-((1-phenyl-1*H*-1,2,3-triazol-4-yl)-methyl)-piperazin-1-yl)-methanone (8a). Brown solid; (82%); mp 99–101 °C; ^{1}H NMR (400 MHz, DMSO-*d*6) δ 8.74 (s, 1H), 8.55 (d, 1H), 7.91 (d, 2H), 7.62–7.57 (m, 3H), 7.48 (t, 1H), 7.41 (dd, 1H), 3.72 (s, 2H), 3.57 (s, 4H), 2.55 (s, 4H), 2.37 (s, 3H). ^{13}C NMR (101 MHz, DMSO-*d*6) δ 161.33, 144.75, 144.26, 143.50, 137.14, 130.33, 129.01, 127.33, 125.01, 122.56, 120.39, 117.34, 116.50, 52.75, 45.14, 15.27. ESI-MS: (*m*/*z*) calcd for $C_{22}H_{22}ClN_7O$: 435.16, found 436.19 $(M + H)^+$; anal. calcd for $C_{22}H_{22}ClN_7O$: (%) C, 60.62; H, 5.09; Cl, 8.13; N, 22.49; O, 3.67. Found: C, 60.57; H, 5.04; Cl, 8.18; N, 22.43; O, 3.71.

(6-Chloro-2-methylimidazo-[1,2-*a*]-pyridin-3-yl)(4-((1-(4-nitrophenyl)-1*H*-1,2,3-triazol-4-yl)-methyl)-piperazin-1-yl)-methanone (8b). Pale yellow solid; (79%); mp 220–221 °C; ^{1}H NMR (400 MHz, DMSO-*d*6) δ 8.97 (s, 1H), 8.58 (s, 1H), 8.49–8.43 (m, 2H), 8.29–8.22 (m, 2H), 7.62 (s, 1H), 7.43 (s, 1H), 3.76 (s, 2H), 3.58 (s, 4H), 2.57 (s, 4H), 2.42–2.33 (m, 3H). ^{13}C NMR (101 MHz, DMSO) δ 170.44, 166.88, 161.56, 148.66, 147.07, 141.38, 127.41, 126.03, 125.25, 123.14, 120.96, 119.91, 117.51, 52.69, 45.01, 43.39, 18.59. ESI-MS: (*m*/*z*) calcd for $C_{22}H_{21}ClN_8O_3$: 480.14, found 481.16 $(M + H)^+$; anal. calcd for $C_{22}H_{21}ClN_8O_3$: (%) C, 54.95; H, 4.40; Cl, 7.37; N, 23.30; O, 9.98. Found: C, 54.90; H, 4.35; Cl, 7.40; N, 23.34; O, 9.93.

(6-Chloro-2-methylimidazo-[1,2-*a*]-pyridin-3-yl)(4-((1-(4-(trifluoromethyl)-phenyl)-1*H*-1,2,3-triazol-4-yl)-methyl)-piperazin-1-yl)-methanone (8c). Off-white solid; (85%); mp 95–97 °C; ^{1}H NMR (400 MHz, DMSO) δ 8.92 (s, 1H), 8.55 (d, 1H), 8.31–8.26 (m, 2H), 7.80–7.89 (m, 2H), 7.60 (d, 1H), 7.41 (dd, 1H), 3.74 (s, 2H), 3.58 (s, 4H), 2.55 (s, 4H), 2.37 (s, 3H). ^{13}C NMR (101 MHz, DMSO-*d*6) δ 161.34, 145.10, 144.56, 143.97, 137.62, 131.76, 127.29, 125.50, 124.28, 122.96, 119.77, 117.37, 117.03, 109.28, 52.77, 52.71, 45.11, 15.28. ESI-MS: (*m*/*z*) calcd for $C_{23}H_{21}ClF_3N_7O$: 503.14, found 504.17 $(M + H)^+$; anal. calcd for $C_{23}H_{21}ClF_3N_7O$: (%) C, 54.82; H, 4.20; Cl, 7.03; F, 11.31; N, 19.46; O, 3.17. Found: C, 54.79; H, 4.25; Cl, 7.07; F, 11.34; N, 19.40; O, 3.12.

(6-Chloro-2-methylimidazo-[1,2-*a*]-pyridin-3-yl)(4-((1-(4-ethylphenyl)-1*H*-1,2,3-triazol-4-yl)-methyl)-piperazin-1-yl)-methanone (8d). Sticky liquid; (74%); ^{1}H NMR (400 MHz, DMSO-*d*6) δ 8.70 (s, 1H), 8.56 (s, 1H), 7.81 (d, 2H), 7.60 (d, 1H), 7.42 (d, 3H), 3.76 (s, 2H), 3.58 (m, 4H), 2.74–2.64 (m, 4H), 2.37 (s, 3H), 1.22 (t, 3H). ^{13}C NMR (101 MHz, DMSO-*d*6) δ 161.50, 144.87, 144.77, 135.11, 129.53, 127.31, 125.17, 122.83, 122.78, 120.46, 119.78, 117.48, 110.47, 52.61, 52.42, 44.76, 28.13, 15.92, 15.46. ESI-MS: (*m*/*z*) calcd for $C_{24}H_{26}ClN_7O$: 463.19, found 464.13 $(M + H)^+$; anal. calcd for $C_{24}H_{26}ClN_7O$: (%) C, 62.13; H, 5.65; Cl, 7.64; N, 21.13; O, 3.45. Found: C, 62.10; H, 5.69; Cl, 7.60; N, 21.16; O, 3.41.

(6-Chloro-2-methylimidazo-[1,2-*a*]-pyridin-3-yl)(4-((1-(4-fluorophenyl)-1*H*-1,2,3-triazol-4-yl)-methyl)-piperazin-1-yl)-methanone (8e). Brown solid; (62%); mp 109–111 °C; ^{1}H NMR (400 MHz, DMSO-*d*6) δ 8.74 (s, 1H), 8.56 (d, 1H), 7.99–7.93 (m, 2H), 7.61 (d, 1H), 7.50–7.38 (m, 3H), 3.79 (s, 2H), 3.59 (s, 4H), 2.77–2.54 (m, 4H), 2.38 (s, 3H). ^{13}C NMR (101 MHz, DMSO) δ 163.26, 161.39, 160.82, 144.68, 143.97, 133.61, 125.05, 123.18, 122.83, 122.75, 119.88, 117.27, 117.04, 52.53, 52.34, 44.65, 15.49, 15.22. ESI-MS: (*m*/*z*) calcd for $C_{22}H_{21}ClFN_7O$: 453.15, found 454.19 $(M + H)^+$; anal. calcd for $C_{22}H_{21}ClFN_7O$: (%) C, 58.22; H, 4.66; Cl, 7.81; F, 4.19; N, 21.60; O, 3.52. Found: C, 58.20; H, 4.63; Cl, 7.79; F, 4.14; N, 21.63; O, 3.56.

(4-((1-(4-Bromophenyl)-1*H*-1,2,3-triazol-4-yl)-methyl)-piperazin-1-yl)(6-chloro-2-methylimidazo-[1,2-*a*]-pyridin-3-yl)-methanone (8f). Off-white solid; (74%); mp 93–95 °C; ^{1}H NMR (400 MHz, DMSO-*d*6) δ 8.78 (s, 1H), 8.55 (s, 1H), 7.90 (d, J = 8.9 Hz, 2H), 7.80 (d, 2H), 7.61 (d, 1H), 7.41 (dd, 2H), 3.72 (s, 2H), 3.57 (s, 4H), 2.53 (s, 4H), 2.34 (s, 3H). ^{13}C NMR (101 MHz, DMSO-*d*6) δ 161.48, 145.05,

138.51, 136.36, 133.21, 127.31, 125.17, 122.80, 122.32, 121.60, 119.82, 117.56, 55.34, 52.74, 45.06, 15.42. ESI-MS: (*m*/*z*) calcd for $C_{22}H_{21}BrClN_7O$: 513.07, found 514.02 $(M + H)^+$; anal. calcd for $C_{22}H_{21}BrClN_7O$: (%) C, 51.33; H, 4.11; Br, 15.52; Cl, 6.89; N, 19.05; O, 3.11. Found: C, 51.37; H, 4.08; Br, 15.55; Cl, 6.83; N, 19.01; O, 3.14.

(6-Chloro-2-methylimidazo-[1,2-*a*]-pyridin-3-yl)(4-((1-(3-nitrophenyl)-1*H*-1,2,3-triazol-4-yl)-methyl)-piperazin-1-yl)-methanone (8g). Pale yellow solid; (86%); mp 222–223 °C; ^{1}H NMR (400 MHz, DMSO-*d*6) *δ* 8.99 (s, 1H), 8.75 (t, 1H), 8.56 (s, 1H), 8.42 (dd, 1H), 8.32 (dd, 1H), 7.89 (dd, 1H), 7.61 (d, 1H), 7.41 (d, 1H), 3.75 (s, 2H), 3.58 (s, 4H), 2.57 (s, 4H), 2.38 (s, 3H). ^{13}C NMR (101 MHz, DMSO-*d*6) *δ* 161.49, 148.99, 145.24, 137.73, 131.9, 127.29, 126.40, 126.06–125.38, 125.01, 123.42, 123.13, 120.13, 119.80, 117.47, 115.05, 52.74, 45.28, 45.07, 15.48. ESI-MS: (*m*/*z*) calcd for $C_{22}H_{21}ClN_8O_3$: 480.14, found 481.19 $(M + H)^+$; anal. calcd for $C_{22}H_{21}ClN_8O_3$: (%) C, 54.95; H, 4.40; Cl, 7.37; N, 23.30; O, 9.98. Found: C, 54.90; H, 4.43; Cl, 7.33; N, 23.33; O, 9.94.

(6-Chloro-2-methylimidazo-[1,2-*a*]-pyridin-3-yl)(4-((1-(3-(trifluoromethyl)-phenyl)-1*H*-1,2,3-triazol-4-yl)-methyl)-piperazin-1-yl)-methanone (8h). Brown solid; (60%); mp 123–125 °C; ^{1}H NMR (400 MHz, DMSO-*d*6) *δ* 8.95 (s, 1H), 8.73 (t, 1H), 8.52 (s, 1H), 8.40 (dd, 1H), 8.36 (dd, 1H), 7.84 (dd, 1H), 7.75 (d, 1H), 7.36 (d, 1H), 3.70 (s, 2H), 3.52 (s, 4H), 2.52 (s, 4H), 2.32 (s, 3H). ^{13}C NMR (101 MHz, DMSO-*d*6) *δ* 161.35, 145.11, 144.76, 143.82, 137.61, 131.74, 127.22, 125.66, 124.46, 122.71, 119.73, 117.47, 117.01, 109.232, 52.75, 52.12, 45.54, 15.22. ESI-MS: (*m*/*z*) calcd for $C_{23}H_{21}ClF_3N_7O$: 503.14, found 504.10 $(M + H)^+$; anal. calcd for $C_{23}H_{21}ClF_3N_7O$: (%) C, 54.82; H, 4.20; Cl, 7.03; F, 11.31; N, 19.46; O, 3.17. Found: C, 54.85; H, 4.23; Cl, 7.00; F, 11.36; N, 19.50; O, 3.21.

(6-Chloro-2-methylimidazo-[1,2-*a*]-pyridin-3-yl)(4-((1-(3-methoxyphenyl)-1*H*-1,2,3-triazol-4-yl)-methyl)-piperazin-1-yl)-methanone (8i). Brown solid; (58%); mp 97–98 °C; ^{1}H NMR (400 MHz, DMSO-*d*6) *δ* 8.77 (s, 1H), 8.55 (s, 1H), 7.60 (d, 1H), 7.49 (d, 3H), 7.41 (d, 1H), 7.04 (s, 1H), 3.86 (s, 3H), 3.72 (s, 2H), 3.57 (s, 4H), 2.54 (d, 4H), 2.37 (s, 3H). ^{13}C NMR (101 MHz, DMSO-*d*6) *δ* 161.34, 160.64, 144.62, 143.99, 138.19, 131.25, 127.29, 125.02, 122.69, 119.77, 117.36, 116.51, 114.72, 112.35, 105.96, 56.06, 52.79, 45.00, 15.29. ESI-MS: (*m*/*z*) calcd for $C_{23}H_{24}ClN_7O_2$: 465.17, found 466.14 $(M + H)^+$; anal. calcd for $C_{23}H_{24}ClN_7O_2$: (%) C, 59.29; H, 5.19; Cl, 7.61; N, 21.04; O, 6.87. Found: C, 59.26; H, 5.22; Cl, 7.65; N, 21.01; O, 6.83.

(6-Chloro-2-methylimidazo-[1,2-*a*]-pyridin-3-yl)(4-((1-(3-chlorophenyl)-1*H*-1,2,3-triazol-4-yl)-methyl)-piperazin-1-yl)-methanone (8j). Pale brown solid; (81%); mp 89–91 °C; ^{1}H NMR (400 MHz, DMSO-*d*6) *δ* 8.84 (s, 1H), 8.56 (s, 1H), 8.06 (s, 1H), 7.94 (d, 1H), 7.67–7.53 (m, 3H), 7.42 (d, 1H), 3.78 (s, 2H), 3.59 (s, 4H), 2.60 (s, 4H), 2.38 (s, 3H). ^{13}C NMR (101 MHz, DMSO-*d*6) *δ* 161.15, 145.11, 144.49, 143.42, 137.58, 131.79, 127.21, 125.46, 124.67, 122.61, 119.41, 117.44, 117.02, 109.78, 52.74, 52.15, 45.54, 15.21. ESI-MS: (*m*/*z*) calcd for $C_{22}H_{21}Cl_2N_7O$: 469.12, found 470.17 $(M + H)^+$; anal. calcd for $C_{22}H_{21}Cl_2N_7O$: (%) C, 56.18; H, 4.50; Cl, 15.07; N, 20.85; O, 3.40. Found: C, 56.22; H, 4.56; Cl, 15.10; N, 20.89; O, 3.44.

(6-Chloro-2-methylimidazo-[1,2-*a*]-pyridin-3-yl)(4-((1-(2-fluorophenyl)-1*H*-1,2,3-triazol-4-yl)-methyl)-piperazin-1-yl)-methanone (8k). Off-white solid; (63%); mp 105–107 °C; ^{1}H NMR (400 MHz DMSO-*d*6) *δ* 8.54 (d, 2H), 7.85 (t, 1H), 7.58 (dd, 4H), 7.44 (dd, 2H), 3.79 (s, 2H), 3.59 (s, 4H), 2.60 (s, 4H), 2.38 (s, 3H). ^{13}C NMR (101 MHz, DMSO-*d*6) *δ* 161.38, 155.44, 152.95, 144.66, 143.83, 131.66, 131.58, 127.32, 126.29, 126.02, 125.23, 125.03, 119.79, 117.70, 117.50, 117.37, 52.69, 52.36, 45.23, 15.28. ESI-MS: (*m*/*z*) calcd for $C_{22}H_{21}ClFN_7O$: 453.15, found 454.10 $(M + H)^+$; anal. calcd for $C_{22}H_{21}ClFN_7O$: (%) C, 58.22; H, 4.66; Cl, 7.81; F, 4.19; N, 21.60; O, 3.52. Found: C, 58.26; H, 4.68; Cl, 7.79; F, 4.16; N, 21.63; O, 3.56.

(6-Chloro-2-methylimidazo-[1,2-*a*]-pyridin-3-yl)(4-((1-(2-chlorophenyl)-1*H*-1,2,3-triazol-4-yl)-methyl)-piperazin-1-yl)-methanone (8l). Off-white solid; (85%); mp 94–96 °C; ^{1}H NMR (400 MHz, DMSO) *δ* 8.55 (s, 1H), 8.49 (s, 1H), 7.77 (d, 1H), 7.70 (d, 1H), 7.62 (m, 3H), 7.42 (d, 1H), 3.82 (s, 2H), 3.59 (s, 4H), 2.62 (s, 4H), 2.37 (s, 3H). ^{13}C NMR (101 MHz, DMSO-*d*6) *δ* 161.05, 154.72, 152.15, 144.62, 142.88, 131.76, 131.91, 127.73, 126.67, 126.73, 124.89, 125.00, 119.21, 117.33, 117.51, 117.46, 52.64, 52.33, 45.24, 15.22. ESI-MS: (*m*/*z*) calcd for $C_{22}H_{21}Cl_2N_7O$: 469.12, found 470.16 $(M + H)^+$; anal. calcd for $C_{22}H_{21}Cl_2N_7O$: (%) C, 56.18; H, 4.50; Cl, 15.07; N, 20.85; O, 3.40. Found: C, 56.21; H, 4.55; Cl, 15.04; N, 20.88; O, 3.36.

(6-Chloro-2-methylimidazo-[1,2-*a*]-pyridin-3-yl)(4-((1-(3-chloro-4-fluorophenyl)-1*H*-1,2,3-triazol-4-yl)-methyl)-piperazin-1-yl)-methanone (8m). Pale yellow solid; (55%); mp 213–215 °C; ^{1}H NMR (400 MHz, DMSO-*d*6) *δ* 8.79 (s, 1H), 8.56 (s, 1H), 8.23 (dd, 1H), 7.98 (m, 1H), 7.68 (t, 1H), 7.61 (d, 1H), 7.42 (d, 1H), 3.72 (s, 2H), 3.57 (s, 4H), 2.54 (d, 4H), 2.38 (s, 3H). ^{13}C NMR (101 MHz, DMSO-*d*6) *δ* 161.41 (s), 158.45 (s), 156.13 (s), 145.20 (s), 134.25 (s), 127.27 (s), 125.23 (d, J = 17.2 Hz), 122.99 (s), 122.66 (s), 121.85–120.93 (m), 119.79 (s), 118.69 (s), 118.47 (s), 52.75 (s), 45.53 (s), 45.26 (s), 15.44 (s). ESI-MS: (*m*/*z*) calcd for $C_{22}H_{20}Cl_2FN_7O$: 487.11, found 488.19 $(M + H)^+$; anal. calcd for $C_{22}H_{20}Cl_2FN_7O$: (%) C, 54.11; H, 4.13; Cl, 14.52; F, 3.89; N, 20.08; O, 3.28. Found: C, 54.15; H, 4.10; Cl, 14.56; F, 3.72; N, 20.02; O, 3.32.

(6-Chloro-2-methylimidazo-[1,2-*a*]-pyridin-3-yl)(4-((1-(3,5-dimethylphenyl)-1*H*-1,2,3-triazol-4-yl)-methyl)-piperazin-1-yl)-methanone (8n). Off-white solid; (58%); mp 100–102 °C; ^{1}H NMR (400 MHz, DMSO-*d*6) *δ* 8.79 (s, 1H), 8.65 (s, 1H), 8.56 (s, 1H), 7.89 (dd, 1H), 7.78 (d, 1H), 7.68 (s, 2H), 7.50 (s, 1H), 3.75 (s, 2H), 3.60 (s, 4H), 2.57 (d, 4H), 2.35 (s, 3H). ^{13}C NMR (101 MHz, DMSO-*d*6) *δ* 161.36, 144.18, 138.81, 137.44, 135.11, 130.82, 127.57, 125.08, 122.75, 121.24, 119.27, 117.67, 117.38, 116.54, 52.51, 45.27, 44.88, 19.91, 15.41 ESI-MS: (*m*/*z*) calcd for $C_{24}H_{26}ClN_7O$: 463.19, found 464.25 $(M + H)^+$; anal. calcd for $C_{24}H_{26}ClN_7O$: (%) C, 62.13; H, 5.65; Cl, 7.64; N, 21.13; O, 3.45. Found: C, 62.10; H, 5.69; Cl, 7.60; N, 21.17; O, 3.40.

(6-Chloro-2-methylimidazo-[1,2-*a*]-pyridin-3-yl)(4-((1-(3,4-dimethylphenyl)-1*H*-1,2,3-triazol-4-yl)-methyl)-piperazin-1-yl)-methanone (8o). Dark brown solid; (56%); mp 101–103 °C; ^{1}H NMR (400 MHz, DMSO-*d*6) *δ* 8.65 (s, 1H), 8.55 (s, 1H), 7.71 (s, 1H), 7.61 (d, 2H), 7.41 (dd, 1H), 7.33 (d, 1H), 3.71 (s, 2H), 3.57 (s, 4H), 2.54 (s, 4H), 2.38 (s, 3H), 2.32 (s, 3H), 2.29 (s, 3H). ^{13}C NMR (101 MHz, DMSO-*d*6) *δ* 161.33, 144.57, 143.98, 138.52, 137.30, 135.10, 130.97, 129.63, 127.29, 125.02, 122.36, 121.25, 119.77, 117.63, 117.37, 116.53, 52.80, 45.06, 44.87, 19.87, 19.41, 15.29. ESI-MS: (*m*/*z*) calcd for $C_{24}H_{26}ClN_7O$: 463.19, found 464.15 $(M + H)^+$; anal.

calcd for $C_{24}H_{26}ClN_7O$: (%) C, 62.13; H, 5.65; Cl, 7.64; N, 21.13; O, 3.45. Found: C, 62.16; H, 5.65; Cl, 7.62; N, 21.16; O, 3.41.

(6-Chloro-2-methylimidazo-[1,2-*a*]-pyridin-3-yl)(4-((1-(4-methoxy-2-nitrophenyl)-1*H*-1,2,3-triazol-4-yl)-methyl)-piperazin-1-yl)-methanone (8p). Pale yellow solid; (58%); mp 104–105 °C; ^{1}H NMR (400 MHz, DMSO-*d*6) δ 8.54 (d, 2H), 7.78 (m, 2H), 7.61 (d, 1H), 7.50 (dd, 1H), 7.42 (d, 1H), 3.95 (s, 3H), 3.81 (s, 2H), 3.59 (s, 4H), 2.55 (s, 4H), 2.38 (s, 3H). ^{13}C NMR (101 MHz, DMSO-*d*6) δ 161.42 (s), 160.69 (s), 145.54 (s), 144.66 (s), 129.36 (s), 128.06 (s), 127.33 (s), 126.28 (s), 125.02 (s), 122.55 (s), 119.86 (d, J = 9.2 Hz), 117.84–117.78 (m), 117.57 (d, J = 34.6 Hz), 116.49 (s), 110.99 (s), 57.08 (s), 52.39 (d, J = 20.4 Hz), 52.17–51.19 (m), 44.77 (s), 15.27 (s). ESI-MS: (*m*/*z*) calcd for $C_{23}H_{23}ClN_8O_4$: 510.15, found 511.10 (M + H)$^+$; anal. calcd for $C_{23}H_{23}ClN_8O_4$: (%) C, 54.07; H, 4.54; Cl, 6.94; N, 21.93; O, 12.53. Found: C, 54.11; H, 4.51; Cl, 6.90; N, 21.96; O, 12.50.

(2,7-Dimethylimidazo-[1,2-*a*]-pyridin-3-yl)(4-(2-(4-propyl-1*H*-1,2,3-triazol-1-yl)-ethyl)-piperazin-1-yl)-methanone (10a). Sticky liquid; (76%); ^{1}H NMR (400 MHz, DMSO) δ 8.42 (s, 1H), 7.86 (d, 1H), 7.47 (d, 1H), 6.84 (d, 1H), 4.59 (s, 1H), 4.44 (s, 1H), 4.38 (s, 1H), 2.78 (t, 2H), 2.62–2.54 (m, 3H), 2.36 (s, 6H), 1.60 (dd, 2H), 1.36–1.20 (m, 2H), 0.89 (t, 3H). ^{13}C NMR (101 MHz, DMSO-*d*6) δ 161.52, 161.86, 147.77, 146.81, 144.25, 127.28, 124.69, 122.26, 119.73, 117.57, 57.21, 52.35, 47.16, 45.84, 31.71, 22.94, 21.09, 15.18, 14.85. ESI-MS: (*m*/*z*) calcd for $C_{21}H_{29}N_7O$: 395.24, found 396.16 (M + H)$^+$; anal. calcd for $C_{21}H_{29}N_7O$: (%) C, 63.77; H, 7.39; N, 24.79; O, 4.05. Found: C, 63.74; H, 7.32; N, 24.75; O, 4.09.

(2,7-Dimethylimidazo-[1,2-*a*]-pyridin-3-yl)(4-(2-(4-nonyl-1*H*-1,2,3-triazol-1-yl)-ethyl)-piperazin-1-yl)-methanone (10b). Sticky liquid; (72%); ^{1}H NMR (400 MHz, DMSO-*d*6) δ 8.38 (d, 1H), 7.75 (s, 1H), 7.43 (s, 1H), 6.88 (d, 1H), 4.36 (t, 2H), 3.45 (s, 4H), 2.72 (t, 2H), 2.47 (s, 4H), 2.40 (t, 2H), 2.35 (s, 6H), 1.72 (m, 2H), 1.32–1.25 (m, 12H) 0.88 (t, 3H). ^{13}C NMR (101 MHz, DMSO-*d*6) δ 161.53, 161.82, 147.73, 146.73, 144.19, 127.38, 124.73, 122.28, 119.69, 117.42, 57.24, 52.45, 47.08, 45.77, 31.68, 29.74–28.62 (m), 25.41, 22.47, 21.08, 15.24, 14.32. ESI-MS: (*m*/*z*) calcd for $C_{27}H_{41}N_7O$: 479.34, found 480.20 (M + H)$^+$; anal. calcd for $C_{27}H_{41}N_7O$: (%) C, 67.61; H, 8.62; N, 20.44; O, 3.34. Found: C, 67.66; H, 8.56; N, 20.84; O, 3.39.

(4-(2-(4-Cyclopropyl-1*H*-1,2,3-triazol-1-yl)-ethyl)-piperazin-1-yl)(2,7-dimethylimidazo-[1,2-*a*]-pyridin-3-yl)-methanone (10c). Sticky liquid; (59%); ^{1}H NMR (400 MHz, DMSO-*d*6) δ 8.42 (s, 1H), 7.84 (s, 1H), 7.41 (s, 1H), 6.85 (d, 1H), 4.40 (t, 2H), 3.51 (s, 4H), 2.77 (t, 2H), 2.52 (s, 4H), 2.36 (s, 6H), 1.96–1.89 (m, 1H), 0.89 (d, 2H), 0.70 (d, 2H). ^{13}C NMR (101 MHz, DMSO) δ 161.91, 149.25, 137.18, 127.86, 126.66, 121.85, 121.65, 115.90, 115.71, 57.19, 52.97, 47.02, 45.03, 21.36, 8.09, 7.01. ESI-MS: (*m*/*z*) calcd for $C_{21}H_{27}N_7O$: 393.23, found 394.35 (M + H)$^+$; anal. calcd for $C_{21}H_{27}N_7O$: (%) C, 64.10; H, 6.92; N, 24.92; O, 4.07. Found: C, 64.13; H, 6.96; N, 24.86; O, 4.01.

(4-(2-(4-(4-(*tert*-Butyl)phenyl)-1*H*-1,2,3-triazol-1-yl)ethyl)-piperazin-1-yl)(2,7-dimethylimidazo-[1,2-*a*]-pyridin-3-yl)-methanone (10d). Pale yellow solid; (63%); mp 148–150 °C; ^{1}H NMR (400 MHz, DMSO-*d*6) δ 8.52 (s, 2H), 7.76 (d, 2H), 7.46 (d, 3H), 6.83 (s, 1H), 4.53 (s, 2H), 3.47 (d, 4H), 2.85 (s, 2H), 2.52 (s, 4H), 2.33 (s, 6H), 1.30 (s, 9H). ^{13}C NMR (101 MHz, DMSO-*d*6) δ 160.98, 154.76, 150.71, 146.58, 136.77, 136.68, 128.60, 126.25, 126.07, 125.39, 121.89, 115.61, 57.15, 52.99, 47.30, 45.06, 34.79, 31.53, 21.44, 15.01. ESI-MS: (*m*/*z*) calcd for $C_{28}H_{35}N_7O$: 485.29, found 486.19 (M + H)$^+$; anal. calcd for $C_{28}H_{35}N_7O$: (%) C, 69.25; H, 7.26; N, 20.19; O, 3.29. Found: C, 69.29; H, 7.32; N, 20.22; O, 3.22.

(6-Chloro-2-methylimidazo-[1,2-*a*]-pyridin-3-yl)(4-(2-(4-propyl-1*H*-1,2,3-triazol-1-yl)-ethyl)-piperazin-1-yl)-methanone (11a). Sticky liquid; (70%); ^{1}H NMR (400 MHz, DMSO-*d*6) δ 8.56 (s, 1H), 7.87 (s, 1H), 7.61 (s, 1H), 7.42 (s, 1H), 4.44 (s, 2H), 3.52 (s, 4H), 2.79 (s, 2H), 2.55 (d, 4H), 2.42 (s, 2H), 2.36 (s, 3H), 1.60 (d, 2H), 0.90 (s, 3H). ^{13}C NMR (101 MHz, DMSO-*d*6) δ 161.28, 161.11, 147.28, 146.81, 144.38, 127.24, 124.61, 122.92, 119.34, 115.31, 57.22, 52.36, 47.33, 45.44, 31.61, 22.09, 15.10, 14.73. ESI-MS: (*m*/*z*) calcd for $C_{20}H_{26}ClN_7O$: 415.19, found 416.26 (M + H)$^+$; anal. calcd for $C_{20}H_{26}ClN_7O$: (%) C, 57.76; H, 6.30; Cl, 8.52; N, 23.57; O, 3.85. Found: C, 57.72; H, 6.26; Cl, 8.57; N, 23.60; O, 3.82.

(6-Chloro-2-methylimidazo-[1,2-*a*]-pyridin-3-yl)(4-(2-(4-nonyl-1*H*-1,2,3-triazol-1-yl)-ethyl)-piperazin-1-yl)-methanone (11b). White solid; (64%); mp 90–92 °C; ^{1}H NMR (400 MHz, DMSO-*d*6) δ 8.55 (d, 1H), 7.86 (s, 1H), 7.61 (d, 1H), 7.42 (d, 1H), 4.44 (t, 2H), 3.51 (s, 4H), 2.79 (t, 2H), 2.59 (t, 2H), 2.37 (s, 4H), 1.66–1.50 (m, 2H), 1.39–1.12 (m, 14H), 0.84 (t, 3H). ^{13}C NMR (101 MHz, DMSO) δ 161.33, 147.12, 144.69, 127.34, 124.97, 122.66, 119.85, 117.41, 57.21, 52.84, 47.04, 44.91, 31.71, 29.41, 29.24, 28.95, 25.42, 22.53, 15.24, 14.39. ESI-MS: (*m*/*z*) calcd for $C_{26}H_{38}ClN_7O$: 499.28, found 500.19 (M + H)$^+$; anal. calcd for $C_{26}H_{38}ClN_7O$: (%) C, 62.45; H, 7.66; Cl, 7.09; N, 19.61; O, 3.20. Found: C, 62.47; H, 7.61; Cl, 7.11; N, 19.57; O, 3.24.

(6-Chloro-2-methylimidazo-[1,2-*a*]-pyridin-3-yl)(4-(2-(4-cyclopropyl-1*H*-1,2,3-triazol-1-yl)-ethyl)-piperazin-1-yl)-methanone (11c). Pale yellow solid; (81%); mp 105–107 °C; ^{1}H NMR (400 MHz, DMSO-*d*6) δ 8.53 (s, 1H), 7.83 (s, 1H), 7.59 (d, 1H), 7.40 (d, 1H), 4.40 (t, 2H), 3.52 (s, 4H), 2.77 (t, 2H), 2.52 (s, 4H), 2.35 (s, 3H), 2.00–1.87 (m, 1H), 0.88 (s, 2H), 0.69 (s, 2H). ^{13}C NMR (101 MHz, DMSO-*d*6) δ 161.30, 149.13, 144.62, 144.00, 127.27, 125.00, 121.49, 119.79, 1187.40, 116.59, 57.22, 52.88, 47.04, 45.24, 15.28, 8.08, 7.02. ESI-MS: (*m*/*z*) calcd for $C_{20}H_{24}ClN_7O$: 413.17, found 414.10 (M + H)$^+$; anal. calcd for $C_{20}H_{24}ClN_7O$: (%) C, 58.04; H, 5.84; Cl, 8.56; N, 23.69; O, 3.87. Found: C, 58.07; H, 5.81; Cl, 8.51; N, 23.73; O, 3.82.

(4-(2-(4-(4-(*tert*-Butyl)-phenyl)-1*H*-1,2,3-triazol-1-yl)-ethyl)-piperazin-1-yl)(6-chloro-2-methylimidazo-[1,2-*a*]-pyridin-3-yl)-methanone (11d). Off-white solid; (72%); mp 187–189 °C; ^{1}H NMR (400 MHz, DMSO-*d*6) δ 8.57 (s, 2H), 7.85 (m, 2H), 7.61 (dd, 1H), 7.40 (m, 4H), 4.56 (t, 2H), 3.54 (s, 4H), 2.88 (t, 2H), 2.55 (s, 4H), 2.37 (s, 3H). ^{13}C NMR (101 MHz, DMSO-*d*6) δ 161.30 (s), 146.61 (s), 144.54 (s), 144.09 (s), 134.61 (s), 131.26 (s), 129.38 (s), 128.30 (s), 127.41 (s), 125.59 (s), 124.97 (s), 122.20 (s), 119.88 (s), 117.34 (s), 57.08 (s), 52.84 (s), 47.31 (s), 45.05 (s), 15.18 (s). ESI-MS: (*m*/*z*) calcd for $C_{23}H_{24}ClN_7O$: 449.17, found 450.25 (M + H)$^+$; anal. calcd for $C_{23}H_{24}ClN_7O$: (%) C, 61.40; H, 5.38; Cl, 7.88; N, 21.79; O, 3.56. Found: C, 61.46; H, 5.36; Cl, 7.92; N, 21.74; O, 3.52.

(4-(2-(4-(4-(*tert*-Butyl)-phenyl)-1*H*-1,2,3-triazol-1-yl)-ethyl)-piperazin-1-yl)(6-chloro-2-methylimidazo-[1,2-*a*]-pyridin-3-yl)-methanone (11e). Off-white solid; (64%); mp 224–226 °C; ^{1}H NMR (400 MHz, DMSO-*d*6) δ 8.54 (s, 1H), 7.82 (s, 1H), 7.60 (d, 1H), 7.50 (d, 2H), 7.44 (d, 1H), 7.33 (d, 2H), 4.50 (s, 2H), 3.42 (d, 4H), 2.88 (s, 2H), 2.55 (s, 4H), 2.30 (s, 3H), 1.25 (s, 9H). ^{13}C NMR (101 MHz, DMSO-*d*6) δ 161.15, 154.78, 150.72, 146.29, 136.73, 136.19, 128.73,

126.79, 126.13, 125.46, 123.87, 121.79, 115.28, 57.15, 52.17, 47.36, 45.73, 34.82, 31.54, 15.02. ESI-MS: (*m*/*z*) calcd for $C_{27}H_{32}ClN_7O$: 505.24, found 506.15 $(M + H)^+$; anal. calcd for $C_{27}H_{32}ClN_7O$: (%) C, 64.08; H, 6.37; Cl, 7.01; N, 19.38; O, 3.16. Found: C, 64.11; H, 6.33; Cl, 7.04; N, 19.43; O, 3.13.

Conflicts of interest

Authors declare that there is no conflict of interest.

Acknowledgements

KVGCS and SM thank DBT, New Delhi [BT/IN/Spain/39/SMl2017-18] for providing financial support. The financial assistance provided by DIST FIST grant (SR/FST/CSI-240/2012), New Delhi is gratefully acknowledged. SS thanks CSIR for providing SRF fellowship. Central analytical lab facilities of BITS Pilani Hyderabad Campus are gratefully acknowledged.

References

1 P. J. Hotez and N. C. Lo, *Neglected Tropical Diseases: Public Health Control Programs and Mass Drug Administration*, Elsevier Inc., 10th edn, 2020.
2 D. Steverding, *Parasites Vectors*, 2017, **10**, 1–10.
3 S. Kapil, P. K. Singh and O. Silakari, *Eur. J. Med. Chem.*, 2018, **157**, 339–367.
4 N. D. Karunaweera and M. U. Ferreira, *Parasitology*, 2018, **145**, 425–429.
5 K. Pandey, B. Pal, V. N. R. Das, K. Murti, C. S. Lal, N. Verma, S. Bimal, V. Ali, R. B. Verma, R. K. Topno, N. A. Siddiqi and P. Das, *Br. J. Dermatol.*, 2017, **177**, 557–559.
6 https://www.who.int/news-room/fact-sheets/detail/trypanosomiasis-human-african-(sleeping-sickness).
7 N. Devi, D. Singh, R. K. Rawal, J. Bariwal and V. Singh, *Curr. Top. Med. Chem.*, 2016, **16**, 2963–2994.
8 S. Chitti, S. R. Singireddi, P. Santosh Kumar Reddy, P. Trivedi, Y. Bobde, C. Kumar, K. Rangan, B. Ghosh and K. V. G. C. Sekhar, *Bioorg. Med. Chem. Lett.*, 2019, **29**, 2551–2558.
9 Y. Yu, Y. Han, F. Zhang, Z. Gao, T. Zhu, S. Dong and M. Ma, *J. Med. Chem.*, 2020, **63**, 3028–3046.
10 B. Zivkovic, E. Morel, D. Joly, G. Perrault, D. J. Sanger and K. G. Llyod, *Pharmacopsychiatry*, 1990, **23**, 108–113.
11 A. Dang, A. Garg and P. V. Rataboli, *CNS Neurosci. Ther.*, 2011, **17**, 387–397.
12 S. Mohana Roopan, S. M. Patil and J. Palaniraja, *Res. Chem. Intermed.*, 2016, **42**, 2749–2790.
13 W. M. Almirante, L. Polo, A. Mugnaini, E. Provinciali, P. Rugarli, A. Biancotti and A. Gamba, *J. Med. Chem.*, 1965, **1125**, 305–312.
14 E. Esposito, E. Mazzon, I. Paterniti, D. Impellizzeri, P. Bramanti and S. Cuzzocrea, *PLoS One*, 2010, **5**, 1–16.
15 L. A. Sorbera, J. Castañer and P. A. Leeson, *Drugs Future*, 2002, **27**, 935–941.
16 W. A. Simon, M. Herrmann, T. Klein, J. M. Shin, R. Huber, J. Senn-Bilfinger and S. Postius, *J. Pharmacol. Exp. Ther.*, 2007, **321**, 866–874.
17 S. Boggs, V. I. Elitzin, K. Gudmundsson, M. T. Martin and M. J. Sharp, *Org. Process Res. Dev.*, 2009, **13**, 781–785.
18 O. Kim, Y. Jeong, H. Lee, S. Hong and S. Hong, *J. Med. Chem.*, 2011, **54**, 2455–2466.
19 A. A. Trabanco, G. Tresadern, G. J. MacDonald, J. A. Vega, A. I. De Lucas, E. Matesanz, A. García, M. L. Linares, S. A. Alonso De Diego, J. M. Alonso, D. Oehlrich, A. Ahnaou, W. Drinkenburg, C. MacKie, J. I. Andrés, H. Lavreysen and J. M. Cid, *J. Med. Chem.*, 2012, **55**, 2688–2701.
20 J. Rether, G. Erkel, T. Anke, J. Bajtner and O. Sterner, *Bioorg. Med. Chem.*, 2008, **16**, 1236–1241.
21 C. Castera-Ducros, L. Paloque, P. Verhaeghe, M. Casanova, C. Cantelli, S. Hutter, F. Tanguy, M. Laget, V. Remusat, A. Cohen, M. D. Crozet, P. Rathelot, N. Azas and P. Vanelle, *Bioorg. Med. Chem.*, 2013, **21**, 7155–7164.
22 C. Fersing, L. Basmaciyan, C. Boudot, J. Pedron, S. Hutter, A. Cohen, C. Castera-Ducros, N. Primas, M. Laget, M. Casanova, S. Bourgeade-Delmas, M. Piednoel, A. Sournia-Saquet, V. Belle Mbou, B. Courtioux, É. Boutet-Robinet, M. Since, R. Milne, S. Wyllie, A. H. Fairlamb, A. Valentin, P. Rathelot, P. Verhaeghe, P. Vanelle and N. Azas, *ACS Med. Chem. Lett.*, 2019, **10**, 34–39.
23 J. J. Allocco, R. Donald, T. Zhong, A. Lee, Y. S. Tang, R. C. Hendrickson, P. Liberator and B. Nare, *Int. J. Parasitol.*, 2006, **36**, 1249–1259.
24 S. Marhadour, P. Marchand, F. Pagniez, M. A. Bazin, C. Picot, O. Lozach, S. Ruchaud, M. Antoine, L. Meijer, N. Rachidi and P. Le Pape, *Eur. J. Med. Chem.*, 2012, **58**, 543–556.
25 S. Haider, M. S. Alam and H. Hamid, *Inflammation Cell Signaling*, 2014, **1**, e95.
26 D. Dheer, V. Singh and R. Shankar, *Bioorg. Chem.*, 2017, **71**, 30–54.
27 S. Vanaparthi, R. Bantu, N. Jain, S. Janardhan and L. Nagarapu, *Bioorg. Med. Chem. Lett.*, 2020, **30**, 127304.
28 S. Narsimha, S. K. Nukala, T. Savitha Jyostna, M. Ravinder, M. Srinivasa Rao and N. Vasudeva Reddy, *J. Heterocycl. Chem.*, 2020, **57**, 1655–1665.
29 I. Baccelli, J. Krosl, G. Boucher, I. Boivin, V. P. Lavallée, J. Hébert, S. Lemieux, A. Marinier and G. Sauvageau, *Blood Cancer J.*, 2017, **7**, e529.
30 E. A. Johnson, R. S. Marks, S. J. Mandrekar, S. L. Hillman, M. D. Hauge, M. D. Bauman, E. J. Wos, D. F. Moore, J. W. Kugler, H. E. Windschitl, D. L. Graham, A. M. Bernath, T. R. Fitch, G. S. Soori, J. R. Jett, A. A. Adjei and E. A. Perez, *Lung Cancer*, 2008, **60**, 200–207.
31 https://clinicaltrials.gov/ct2/show/NCT00003869Title.
32 K. Das, J. D. Bauman, A. S. Rim, C. Dharia, A. D. Clark, M. J. Camarasa, J. Balzarini and E. Arnold, *J. Med. Chem.*, 2011, **54**, 2727–2737.
33 S. G. Agalave, S. R. Maujan and V. S. Pore, *Chem.–Asian J.*, 2011, **6**, 2696–2718.
34 W. H. Mudd and E. P. Stevens, *Tetrahedron Lett.*, 2010, **51**, 3229–3231.

35 T. B. Cassamale, E. C. Costa, D. B. Carvalho, N. S. Cassemiro, C. C. Tomazela, M. C. S. Marques, M. Ojeda, M. F. C. Matos, S. Albuquerque, C. C. P. Arruda and A. C. M. Baroni, *J. Braz. Chem. Soc.*, 2016, **27**, 1217–1228.

36 P. Dwivedi, K. B. Mishra, B. B. Mishra, N. Singh, R. K. Singh and V. K. Tiwari, *Glycoconjugate J.*, 2015, **32**, 127–140.

37 A. Tahghighi, S. Razmi, M. Mahdavi, P. Foroumadi, S. K. Ardestani, S. Emami, F. Kobarfard, S. Dastmalchi, A. Shafiee and A. Foroumadi, *Eur. J. Med. Chem.*, 2012, **50**, 124–128.

38 T. T. Guimarães, M. D. C. F. R. Pinto, J. S. Lanza, M. N. Melo, R. L. Do Monte-Neto, I. M. M. De Melo, E. B. T. Diogo, V. F. Ferreira, C. A. Camara, W. O. Valença, R. N. De Oliveira, F. Frézard and E. N. Da Silva Júnior, *Eur. J. Med. Chem.*, 2013, **63**, 523–530.

39 M. M. Masood, P. Hasan, S. Tabrez, M. B. Ahmad, U. Yadava, C. G. Daniliuc, Y. A. Sonawane, A. Azam, A. Rub and M. Abid, *Bioorg. Med. Chem. Lett.*, 2017, **27**, 1886–1891.

40 C. M. Horn, J. Aucamp, F. J. Smit, R. Seldon, A. Jordaan, D. F. Warner and D. D. N'Da, *Med. Chem. Res.*, 2020, **29**, 1387–1399.

41 M. Shaquiquzzaman, G. Verma, A. Marella, M. Akhter, W. Akhtar, M. F. Khan, S. Tasneem and M. M. Alam, *Eur. J. Med. Chem.*, 2015, **102**, 487–529.

42 F. Alireza, H. Adibi, S. K. Ardestani, S. Shirooie, A. Bozorgomid and A. Jafari, *Iran. J. Pharm. Sci.*, 2017, **16**, 904–909.

43 B. Carlos, A. Pabón, S. Galiano, S. Pérez-Silanes, G. Gonzalez, C. Deyssard, A. Monge, E. Deharo and I. Aldana, *Molecules*, 2012, **17**, 9451–9461.

44 B. M. Fardmoghadam, F. Poorrajab, S. K. Ardestani, S. Emami, A. Shafiee and A. Foroumadi, *Bioorg. Med. Chem.*, 2008, **16**, 4509–4515.

45 C. Subhash, P. Ashok, R. M. Reguera, M. Y. Perez-Pertejo, R. Carbajo-Andres, R. Balana-Fouce, K. V. G. C. Sekhar and M. Sankaranarayanan, *Exp. Parasitol.*, 2018, **189**, 49–60.

46 Z. Wu, Y. Lu, L. Li, R. Zhao, B. Wang, K. Lv, M. Liu and X. You, *ACS Med. Chem. Lett.*, 2016, **7**, 1130–1133.